ELSEVIER

**COORDINATION
CHEMISTRY
REVIEWS**

Limitations of the polyhedral skeletal electron pair theory in organometallic cluster chemistry: examples in tri- and tetrametallic systems

Jean-François Halet

*Laboratoire de Chimie du Solide et Inorganique Moléculaire, URA CNRS 1495, Université de Rennes I,
Avenue du Général Leclerc, 35042 Rennes Cedex, France*

Contents

Abstract

The Polyhedral Skeletal Electron Pair Theory (PSEP) which correlates the structural arrangement of clusters to their electron count does much for rationalizing the structures of a wide range of organometallic clusters. However, these rules based on the isolobal analogy

principle apply less successfully to complicated compounds containing a heteronuclear core. Different tri- and tetranuclear organometallic compounds serve to illustrate some of the limitations of the PSEP theory to account for skeletal isomerism, isomer interconversion or unexpected geometries. Molecular orbital calculations are used to help and sometimes to circumvent some of these limitations.

List of abbreviations

AO	atomic orbital
Bu	butyl, C_4H_9
Cp	cyclopentadienyl, C_5H_5
Cp*	pentamethylcyclopentadienyl, C_5Me_5
CVE	cluster valence electron
Cy	cyclohexyl, C_6H_{11}
dmpe	1,2-bis(dimethylphosphino)ethane, $Me_2PC_2H_4PMe_2$
dppe	1,2-bis(diphenylphosphino)ethane, $Ph_2PC_2H_4PPh_2$
dppm	1,2-bis(diphenylphosphino)methane, $Ph_2PCH_2PPh_2$
dppt	5,6-diphenyl-3-(pyridine-2-yl)-1,2,4-triazine
E	main group element
EAN	effective atomic number
EH	extended Hückel
EPR	electron paramagnetic resonance
Et	ethyl, C_2H_5
FH	Fenske-Hall
FMO	frontier molecular orbital
HOMO	highest occupied molecular orbital
L	two-electron ligand
LUMO	lowest unoccupied molecular orbital
M	transition metal element
Me	methyl, CH_3
MO	molecular orbital
NMR	nuclear magnetic resonance
Ph	phenyl, C_6H_5
py	pyridine, C_5H_5N
Pr	propyl, C_3H_7
PSEP	polyhedral skeletal electron pair
SEP	skeletal electron pair
Tol	tolyl, C_6H_4Me
TSH	tensor surface harmonic

1. Introduction

Being isoelectronic the mixed bismuth–ruthenium $Ru_4(CO)_{12}Bi_2$ and bismuth-osmium $Os_4(CO)_{12}Bi_2$ species are likely to adopt the same geometry. Indeed, in agreement with the so-called PSEP theory which correlates the structural arrangement of a cluster to its electron count [1], their M_4Bi_2 cluster cores both adopt a *closo*-octahedral arrangement consistent with their 7 SEPs [2]. However, they display different skeletal isomeric structures. In the ruthenium species the metal atoms define a square capped above and below by Bi atoms (1) with no direct bismuth-bismuth interaction. On the other hand, the metal atoms in the osmium compound form a butterfly arrangement spanned by a Bi_2 dumb-bell (2). These two compounds characterized by Lewis et al. some years ago [2] illustrate one of the limitations of the PSEP theory. Such an electron-counting theory provides no information on differentiating one skeletal isomer from another.

1   **2**
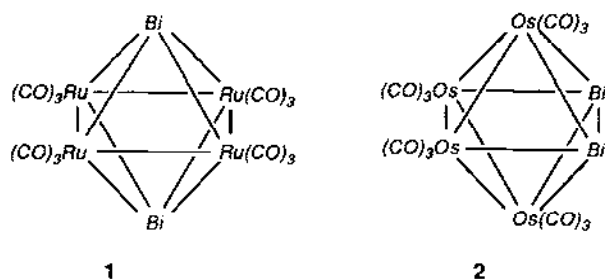
Another limitation of the PSEP theory concerns its breakdown when applied to particular organometallic cluster compounds where the bonding requirements (electronegativity and overlap) of the different elements constituting the cluster core are quite dissimilar, as exemplified by Dahl's 8-SEP compound $Co_4(CO)_{10}(\mu_4\text{-}PPh)_2$ (3) [3]. With such an electron count, the PSEP rules predict a *nido* open octahedron for the Co_4P_2 core. A *closo* octahedron is actually observed analogous to that of the 7-SEP species $Ru_4(CO)_{12}(\mu_4\text{-}Bi)_2$, in disagreement with the PSEP theory.

3
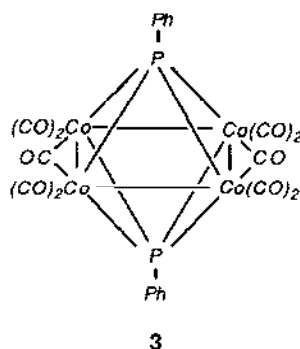
We propose in this review article to explore some of the limitations of the PSEP theory by looking in detail at some particular organometallic families of mixed main

group–transition metal compounds such as those we have just mentioned. This is underpinned by molecular orbital results when available. But before proceeding further, let us acquaint the reader first with the essential features of the PSEP theory.

2. The polyhedral skeletal electron pair theory

Despite the vast structural variety of organometallic cluster compounds characterized during these last decades, general patterns have emerged rapidly enough which have allowed the development of theoretical localized and delocalized descriptions of the bonding in these compounds [1,4]. Today, the delocalized bonding scheme known as the PSEP theory (sometimes called the Wade–Mingos rules), first introduced in 1973 by Mingos et al. [1], is probably the most popular bonding pattern used. It has proven to be particularly powerful for rationalizing or predicting the geometrical structure of a plethora of organometallic cluster compounds which do not conform to the EAN formalism.

Simply stated the PSEP theory relates the structural arrangement of a cluster with its number of CVEs in which are included those involved in skeletal bonding (the so-called skeletal electron pairs [6]). Initially deduced from boron hydride deltahedral structures [5,6], these electron-counting rules were rapidly extended to transition metal clusters [7] using the powerful concept of the isolobal analogy, which connects conical metallic fragments ($M(CO)_3$, $M(Cp)...$) to main group entities (BH, $CH...$) having the same number of frontier molecular orbitals (FMO) of the same symmetry at the same energy [8]. *Closo* (for "closed") metallic arrangements based upon n vertex deltahedra are expected to possess $(14n + 2)$ CVEs or $(n + 1)$ SEPs. The removal of one or two cluster vertices leads to more open geometries, the *nido* (for "nest-like") and the *arachno* (for "web-like") structures, respectively. The appropriate count is $(14n + 4)$ CVEs or $(n + 2)$ SEPs and $(14n + 6)$ CVEs or $(n + 3)$ SEPs for the *nido* and *arachno* forms, respectively. Successive addition of electron pairs to a *closo* cluster results generally in an opening out of the structure to yield *nido* and *arachno* geometries. A pictorial summary of these rules is given in Fig. 1.

The isolobal analogy principle [8] finds particular application in mixed compounds containing varying combinations of main group and transition metal atoms. As shown in Fig. 2, the conical C_{3v} $[Os(CO)_3]^-$ fragment is isolobal to a CH entity or a "bare" Bi atom. They all possess a set of three frontier orbitals in which are housed three electrons susceptible to participating in the cluster bonding in a given compound [8]. Therefore, if in a transition-metal cluster one $[Os(CO)_3]^-$ fragment is replaced by a CH unit, the resulting complex is expected to be isostructural to its homonuclear parent. It will possess the same number of SEPs, but ten less CVEs since the six "t_{2g}" nonbonding and six metal-ligand bonding electrons are replaced by two C–H bonding electrons (see Fig. 2). For instance, $[Os_6(CO)_{18}]^{2-}$ (4) [9], $Os_4(CO)_{12}(\mu_4-C_2H_2)$ (5) [10] and $Os_4(CO)_{12}(\mu_4-Bi_2)$ (2) [2] adopt an octahedral geometry consistent with their electron count of seven skeletal pairs. Note that the total valence electron count of compounds 2 and 5 (66 CVEs) drops by 20 compared
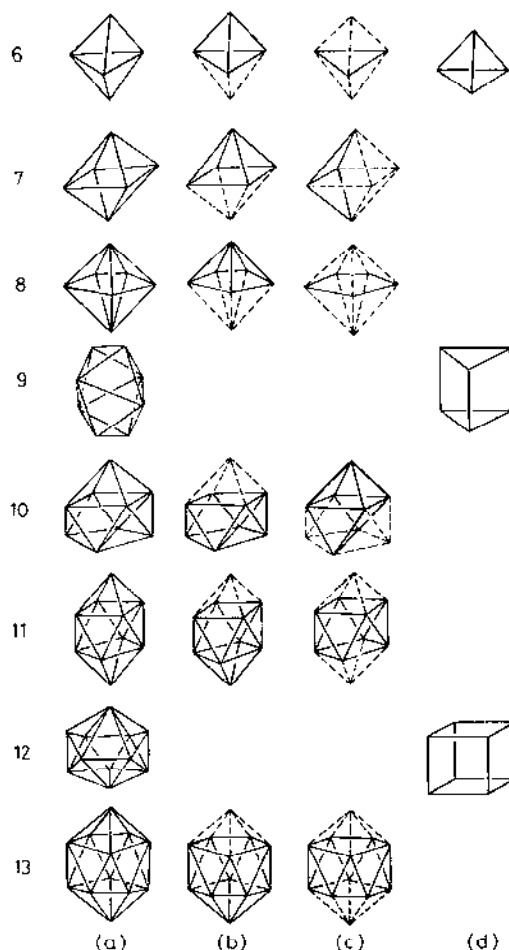
Fig. 1. Examples of *closo* (a), *nido* (b), *arachno* (c) deltahedral and three-connected (d) polyhedra. The number of skeletal electron pairs is given on the left. Only one skeletal isomer is shown for *nido* and *arachno* deltahedra.

to that of compound **4** (86 CVEs) because of the substitution of two $[Os(CO)_3]^-$ units by two main group entities.

Originally developed for rationalizing deltahedron compounds made of conical fragments, the PSEP rules have rapidly been extended to complexes made of nonconical entities (ML_2, CH_2...) [11] and other classes of polyhedral clusters such as the three-connected polyhedral metallic molecules [12]. Moreover, other formalisms such as the capping principle [13] or the principles of polyhedral condensation [14] and polyhedral inclusion [15] have been added to complement the polyhedral skeletal electron pair approach in order to rationalize more complicated cluster compounds. The capping principle demonstrates that capping an edge or a face of a cluster does not change the number of SEPs and modify the count of CVEs of 12.
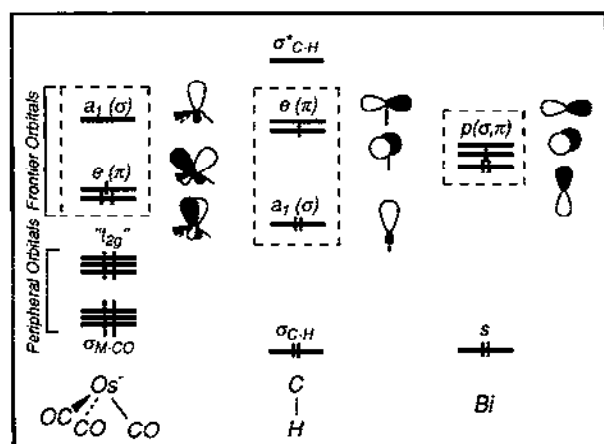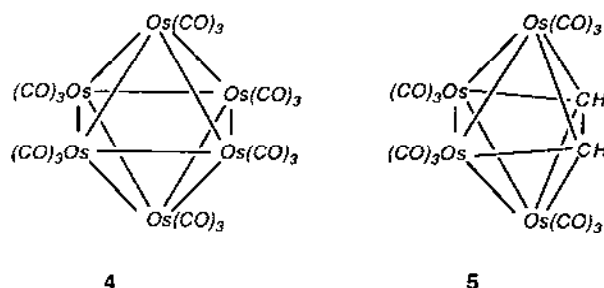
Fig. 2. Comparison of the frontier orbitals of some isolobal fragments.

4   **5**

This is due to a symmetry match between FMOs of the capping unit and those of the parent cluster [13]. The principle of polyhedral condensation allows evaluation of the cluster valence electron count for clusters regarded as the agregation of polyhedra sharing a vertex, an edge or a face. For a given condensed cluster, its total electron count is equal to the sum of the electron counts for the parent polyhedra minus the one characteristic of the shared unit [14]. The principle of inclusion concerns high nuclearity compounds which can be considered as formed of an inner and an outer polyhedron [15].

The PSEP rules have been elegantly justified by the TSH theory formulated by Stone [16]. Considering that all the atoms of a deltahedral cluster lie on a single spherical surface, this methodology derives approximate MOs from the nodal properties of the spherical harmonics which are the solutions to the Schrödinger equation for an electron moving in a spherical potential shell. In practice it allows classification of cluster MOs according to their nodal characteristics (radial (σ-type) and tangential (π- and δ-type)). For a *closo* transition metal cluster M_nL_m for instance, the TSH theory identifies $2n-1$ MOs which should be vacant, leaving $7n+1$ MOs which can be occupied, in agreement with the $14n+2$ electron rule.

Despite the widespread success of the PSEP theory for rationalizing the geometri-

cal features of numerous compounds, the few examples mentioned at the beginning illustrate some of its main limitations, which concern the skeletal isomerism and the deviation from the usual number of skeletal electron pairs for a given cluster compound even made of conical fragments [1]. This is actually associated with the limitations of the isolobal analogy, which does not make any chemical difference between isolobal fragments. In order to circumvent these limitations, numerous theoretical studies using quantum-mechanical calculations have been performed. The largest part of these theoretical works have been published within the EH formalism [17]. In spite of its limitations such as the difficulty in optimizing bond distances or the treatment of open-shell configurations, this one-electron non-self-consistent method has proven to be very effective for rationalizing the structures and the reactivity of organometallic compounds. Its success is due to the possibility of rapidly providing sets of results which can be directly interpretable in terms of perturbation theory through the interaction between frontier orbitals of molecular fragments.

3. Skeletal isomerism and fluxionality in trimetal–alkyne (or alkyne-like) clusters

In cluster chemistry the respective stability of skeletal isomers and the possibility of their interconversion cannot be fully explained using only the PSEP theory. In the case of boranes, for which diamond–square–diamond rearrangement mechanisms often operate, Mingos and Wales have demonstrated the usefulness of the TSH theory for distinguishing orbital symmetry-allowed from orbital symmetry-forbidden processes [1e]. In transition metal or mixed main group–transition metal clusters, the surrounding ligands and/or the heteronuclear nature of the cluster core generally lower the symmetry of the cluster. Consequently, the orbital symmetry selection rules used for boranes lose somewhat their validity and lower barriers for "forbidden" fluxional processes are anticipated. We illustrate this point here with the trimetallic–alkyne M_3C_2 compounds.

3.1. Heterotrimetallic–alkyne complexes

A vast amount of work has been devoted to metal–alkyne clusters [18]. The PSEP theory supported by molecular orbital calculations has proven to be very helpful for understanding their structural chemistry. Trimetallic–alkyne cluster complexes, for instance, are mainly encountered in two distinct geometries depending on their electron counts. Species characterized by 52 CVEs, or 46 "metallic" electrons, or 6 SEPs adopt a *closo*-trigonal-bipyramidal structure with the alkyne moiety lying perpendicular to one metal–metal bond (μ_3-η^2-($\perp$)) mode [19]) such as $Fe_3(CO)_9(\mu_3$-($\perp$)-$C_2Ph_2)$ (6) [20]. The others possessing 54 CVEs, or 48 "metallic" electrons, or 7 SEPs, describe a *nido*-square-pyramidal geometry with the acetylenic ligand positioned parallel to a metal–metal vector (μ_3-η^2-(II) mode [19]) as exemplified by $Co_2Fe(CO)_9(\mu_3$-(II)-$C_2Et_2)$ (7) [21,22]. The electronic structure of these

M_3C_2 compounds, which has been extensively studied previously, shows that in each case the favored geometry, *closo* or *nido*, gives rise to a large HOMO–LUMO gap only for the observed electron count [23–28] (see Fig. 3).

6

7   **8**
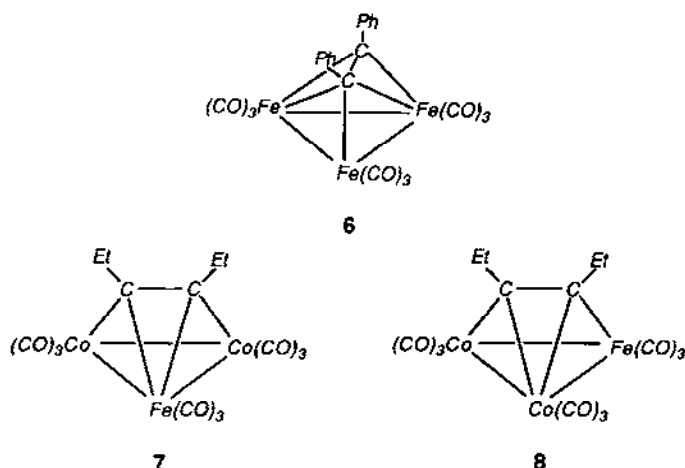
As stated previously, when different kinds of metal atoms are present in a cluster compound the PSEP procedure allows the same electron count for several isomers
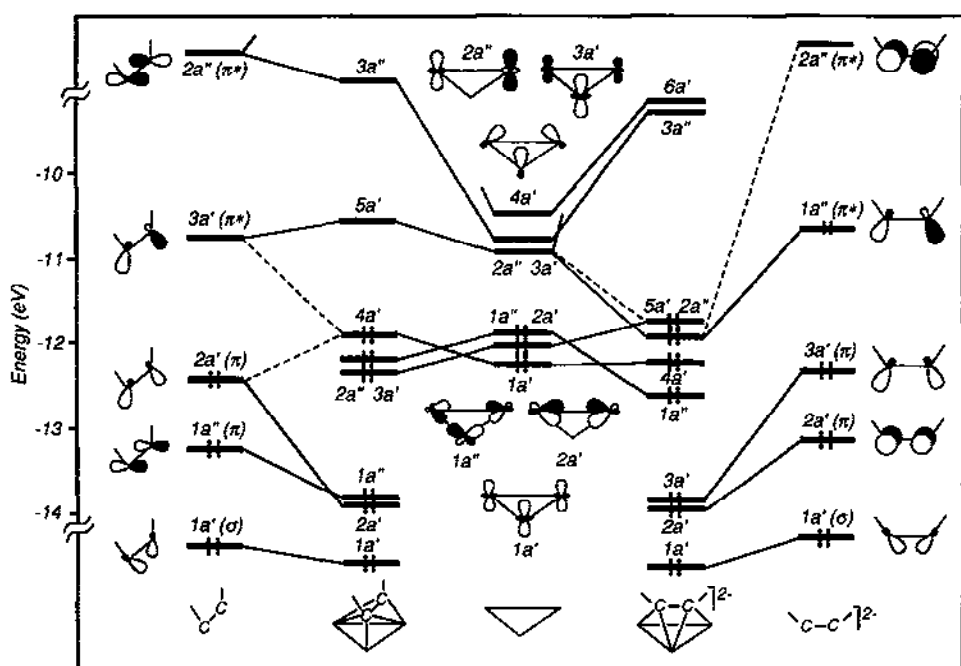

Fig. 3. Interaction diagram of the model $Fe_3(CO)_9(C_2H_2)$ in the 6-SEP *closo* geometry (on the left) and the 7-SEP *nido* geometry (on the right).

which a priori should be of equal stability. This is the case for $Co_2Fe(CO)_9(\mu_3$-(II)-$C_2Et_2)$, which could exist in two *nido* isomeric forms, (7) and (8). Only the symmetrical form (7) is found, at least by X-ray crystallography [21]. Indeed, most of the *closo* and *nido* heterotrimetallic–alkyne species which have been characterized exhibit only one skeletal isomer (see Table 1). It is beyond the capabilities of the PSEP theory to favor one isomer over the other. Note that the favored geometries are not necessarily those which are symmetrical or those which satisfy the 18-electron rule. This is nicely exemplified by the *nido* compound $FeNiMo(Cp)_2(CO)_5(\mu_3$-PhC_2CO_2-*i*-Pr) (9), in which the Mo atom occupies the apical vertex of the square pyramid, leading formally to Fe, Ni and Mo atoms with 17, 18 and 19 electrons, respectively [33]. Coupling with EH calculations is then useful in order to trace and analyze the tiny electronic differences between the different isoelectronic isomers.

Table 1
Selected structurally characterized *closo* and *nido* heterotrimetallic -alkyne compounds

Compound	Apical vertex[a]	d(C−C) (Å)	Remarks	Ref.
6-SEP *closo* clusters				
$Fe_2Ru(CO)_9(C_2Ph_2)$	Ru	1.413(20)		25
$FeW_2(Cp)_2(O)(CO)_5(C_2Tol_2)$	W	1.441(11)		29
$FeW_2(Cp)_2(CO)_6(C_2Tol_2)$	W	1.399(9)	*sb*CO[b]	29,30
7-SEP *nido* clusters				
$FeCo_2(CO)_9(C_2Et_2)$	Fe	1.37(1)		21
$FeCo_2(CO)_8(PPh_3)(C_2Et_2)$	Co	1.367(8)		31
$[FeNi(Cp)(CO)_6(C_2Ph_2)]^-$	Fe	1.383(7)		32
$FeCoNi(Cp)(CO)_6(PhC_2CO_2$-*i*-Pr)	Fe	1.376(8)		33
$FeCoNi(Cp)(CO)_6(C_2Et_2)$	Fe	1.371(7)		34
$FeCoNi(Cp)(CO)_6(PPh_3)(C_2Ph_2)$	Co	1.34(2)		34
$FeNi_2(Cp)_2(CO)_3(C_2Ph_2)$	Fe	1.34(2)		35
$FeNi_2(Cp)_2(CO)_3(PhC_2CO_2$-*i*-Pr)	Fe	1.363(4)		33
$FeNiMo(Cp)_2(CO)_5(PhC_2CO_2$-*i*-Pr)	Mo	1.38(2)		33
$FeMoRu(Cp)(CO)_8(H)(C_2Me_2)$	Mo	1.37(2)		36
$Co_2Ru(CO)_9(C_2Ph_2)$	Co	1.370(3)	*sb*CO	37
$Co_2Ru(CO)_8(PPh_3)(C_2Ph_2)$	Co	1.33(2)	*sb*CO	38
$CoNiRu(Cp)(CO)_6(C_2Ph_2)$	Co	1.377(9)	*sb*CO	34
$Ni_2Ru(Cp)_2(CO)_3(C_2Ph_2)$	Ru	1.40(3)		35
$NiRu_2(Cp)_2(CO)_4(C_2Ph_2)$	Ru	1.383(7)		39
$Fe_2Ir(CO)_8(PEt_3)(PhC_2PEt_3)$	Fe	1.48(1)		40
$Fe_2Ir(CO)_7(PPh_3)_2(PhC_2C_2Ph)$	Fe	1.40(2)		40
$CoNiOs(Cp)(CO)_6(C_2Ph_2)$	Co	1.377(10)	*sb*CO	34
$W_2Os(Cp)_2(CO)_7(C_2Tol_2)$	Os	1.47(3)		
	W	1.43(3)	*sb*CO	30
$W_2Os(Cp)_2(CO)_7(C_2Tol_2)$	Os	1.463(28)		
	W	1.424(29)	*sb*CO	41

[a] Metal atom occupying one of the apical vertices of the closo trigonal bipyramid or the apical vertex of the nido square pyramid. [b] *sb*CO: semi-bridging carbonyl ligand.
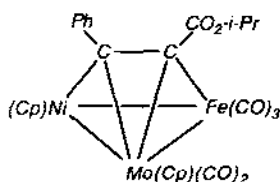
9

EH results performed on the 7-SEP *nido* model $[Fe_3(CO)_9(\mu_3\text{-}C_2H_2)]^{2-}$ indicate that the basal Fe atoms are more negatively charged than the apical one [26]. Consequently, the substitution of an iron center by a more electronegative metal is suspected to occur at the basal sites. It turns out that the replacement of a $Fe(CO)_3$ fragment by a more electronegative metallic group such as $Co(CO)_3$ modifies substantially the extent of localization of the FMOs of the metal triangle and therefore changes the electronic character of the interactions with the capping alkyne ligand. Particularly, a comparison of the nature of the acceptor FMOs of a′ symmetry (3a′ and 4a′ in the middle of Fig. 3) of the $Fe_3(CO)_9$ and $[FeCo_2(CO)_9]^{2+}$ fragments indicates that they are more heavily weighted towards the $Fe(CO)_3$ group than the $Co(CO)_3$ ones in the latter [26,42]. Inversely, the 2a″ acceptor metallic orbital is strongly localized on the Co atoms. Consequently, a stronger interaction between the metallic entity and the organic moiety results if the $Fe(CO)_3$ fragment occupies the apical vertex of the $M_2M'C_2$ square pyramid. In other words σ-bonding to the more electronegative metal centers and π-bonding to the less electronegative metal center will enhance the electron donation from the alkyne ligand towards the metal triangle, favoring thus this isomer. This electron donation accompanied by some back-donation from the metallic framework into the organic unit is responsible for the important lengthening of the C–C vector (typically 1.3–1.5 Å) of the complexed alkyne ligand with respect to the free ligand (1.189 Å).

Most of the reported X-ray structures conform to this pattern, which seems to indicate that the orientation of the alkyne group in the *nido* heterotrimetallic–alkyne complexes depends on the electron-accepting properties of the metallic fragments (see Table 1). The few exceptions in which the less electronegative metallic fragment (according to Allred–Rochow electronegativity values [43]) occupies a basal site rather than the expected apical one concern clusters having the metal triangle made partially or totally of heavier transition metal elements. In this case, one carbonyl ligand attached to the apical metal center is semi-bridged to the electron-deficient basal metallic center (see Table 1). Let us remark that the C–C bond separations of the alkyne group in those exceptions are slightly shorter than the ones measured in comparable compounds. This reflects a smaller interaction with the metallic array (see Table 1). No calculations are available yet in order to fully rationalize the preferred isomer for this type of cluster.

The alkyne orientation within the organometallic skeleton of these *nido* species is very sensitive, since the substitution of a carbonyl by a phosphine on one cobalt center in $FeCo_2(CO)_9(\mu_3\text{-}(II)\text{-}C_2Et_2)$ is sufficient to obtain the other isomer (8) in

the crystal [31]. The same phenomenon is observed for $FeCoNi(Cp)(CO)_6(\mu_3$-(II)-$C_2Et_2)$ [34]. Two isomers for $W_2Os(Cp)_2(CO)_7(\mu_3$-(II)-$C_2Tol_2)$ (**10a** and **b**) have been established by X-ray diffraction [30,41]. Indeed, the EH computed energy differences between the different model isomers are rather small [25]. Moreover, it is worthy of mention that NMR experiments have shown that several isomers interconvert in solution [30,33,34,44].

10
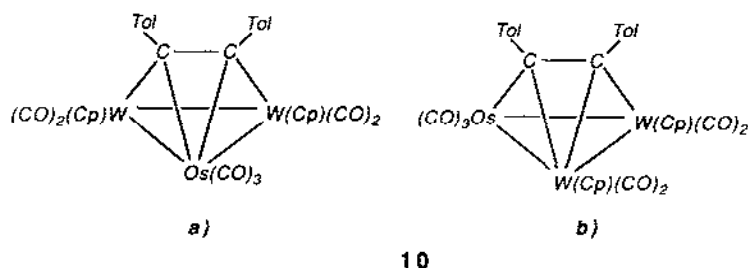
The isomer interconversion is attributed to a fluxional behavior of the alkyne ligand on the metal triangular entity. It is beyond the capabilities of the PSEP theory to predict an interconversion mechanism. According to McGlinchey and colleagues [33,42,45], a mechanism in which the alkyne ligand circumambulates the periphery of the metallic triangle proceeding via *closo* trigonal bipyramidal geometries (unstable for the count of 7 SEPs) is highly energetic and should be ruled out [46]. They propose rather a mechanism of vertex migration over the *nido*-octahedral geometry depicted by the $M_2M'C_2$ core. This is illustrated for $FeNiMo(Cp)_2(CO)_5(\mu_3$-PhC_2CO_2-i-Pr) in (**11**) [33,45]. Such a rearrangement mechanism leading to the racemization of the cluster, sometimes called a square→diamond, diamond→square process [1e], was suggested a long time ago by Stohrer and Hoffmann for the skeletal isomerization of $[C_5H_5]^+$ [47], and appears to be fully analogous to the "windshield wiper" motion that Schilling and Hoffmann proposed to account for the fluxional behavior of alkyne ligands on triangular homometallic surfaces [23].

As for the 7 SEPs *nido* heterotrimetallic $M_2M'C_2$ compounds, only one isomer is generally observed in the crystal for the 6-SEPs *closo* ones. Though the *closo* arrangement is rather scarce (see Table 1), it seems that the preferred isomer isolated in the solid state is also governed by electronic driving forces. According to Fig. 3, and knowing that the replacement in the $Fe_3(CO)_9$ entity of a $Fe(CO)_3$ fragment by a less electronegative metallic unit such as $Ru(CO)_3$ (following Allred–Rochow electronegativity values [43]) enhances the localization of the latter in the symmetrical acceptor FMOs, the interaction between the alkyne moiety and the metal triangle is maximized when the alkyne is σ-bound to the Ru center and π-bound to the Fe centers [25]. Consequently, if the optimization of the electron donation from the alkyne towards the metallic entity plays the major role in the preference of one isomer relative to the other, the less electronegative metallic fragment should occupy one of the apical sites of the trigonal bipyramidal cluster. The three examples reported so far are in agreement with this statement (see Table 1).
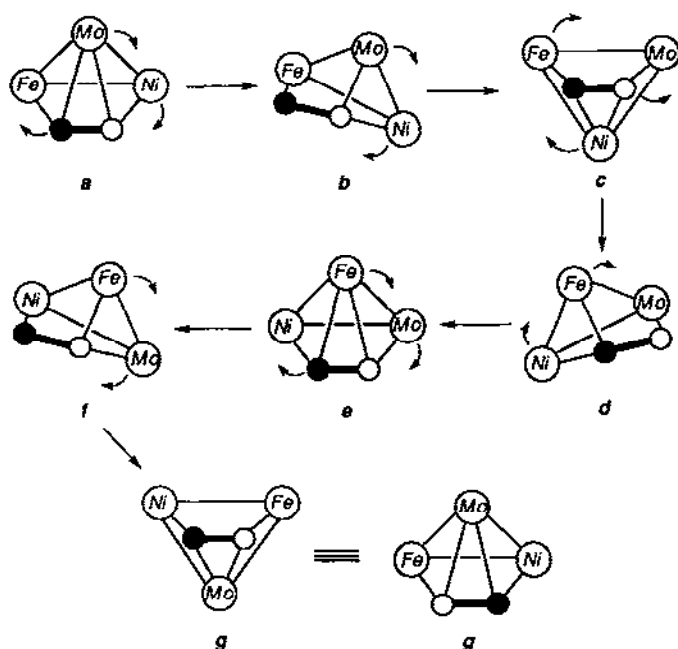
11

3.2. Homotrimetallic–alkyne complexes

A variation of the ligand environment of the atoms constituting the metal triangle in the homotrimetallic–alkyne clusters can also lead to the possibility of several isomers. However, as generally observed in the case of the heterotrimetallic–alkyne complexes, only one isomer exists in the crystal. This is nicely exemplified by the compound $Fe_3(Cp)_2(\mu_3\text{-}CO)(\mu\text{-}CO)(CO)_3(\mu_3\text{-}\eta^2\text{-}(II)C_2(CF_3)_2)$, characterized by Pétillon et al. [48], which exists in two isomeric forms (one symmetrical (12) and one asymmetrical (13)). Only the former (13) has been isolated in the solid state. Nevertheless, the observation of different concentrations of (12) and (13) in different solvents (7 (13) : 1 (12) in CD_2Cl_2 and 13 (13) : 1 (12) in CD_3CN) suggests an equilibrium between (12) and (13) in solution, with the asymmetrical isomer (13) slightly more stable energetically than the symmetrical one (12). According to the authors, the equilibrium is reached over several days [48,49]. Surprisingly, this leads them to conclude that the (13)→(12) interconversion ought to be very slow and should occur via a circumambulation of the alkyne ligand over the metallic triangle with a high interconversion barrier [46], rather than via the least-motion pathway described above (see (11)) [33,45]. The replacement of CO by a better σ-donor ligand emphasizes the preference for the asymmetrical isomer (13) in solution. For instance, the thermal substitution of a tertiary phosphite such as $P(OMe_3)$ for CO leads to the formation of $Fe_3(Cp)_2(CO)_4(P(OMe_3))(\mu_3\text{-}(II)\text{-}C_2(CF_3)_2)$ with an asymmetrical:symmetrical ratio very high compared to that of $Fe_3(Cp)_2(CO)_5(\mu_3\text{-}(II)\text{-}$

$C_2(CF_3)_2$) parent compound (49:1 versus 7:1 in CD_2Cl_2, respectively). With a
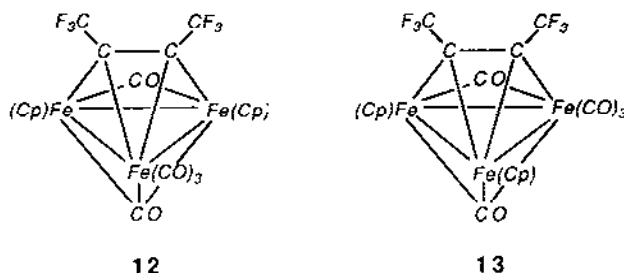
tertiary phosphine such as PMe_3 only the asymmetrical isomer of $Fe_3(Cp)_2(CO)_4(PMe_3)(\mu_3$-(II)-$C_2(CF_3)_2$) is obtained in solution [49].

These observations contrast somewhat with previous theoretical analyses, which predict a slight preference for the symmetrical conformer for the 7-SEP *nido* $[Fe_3(Cp)_2(CO)_3(\mu_3$-(II)-$C_2H_2)]^{4-}$ model (14) [26]. In order to try to understand the preference of the symmetrical form (14) over the asymmetrical one (15), we have to dwell on some of the differences between $Fe(CO)_3$ and $[Fe(Cp)]^-$, although they are isolobal fragments exhibiting remarkably similar bonding properties [8]. As illustrated in Fig. 4 the differences concern mainly the shape and the energy of their σ-type (a_1) and π-type (e) frontier orbitals. The a_1 FMO in $[Fe(Cp)]^-$ is nearly a pure hybrid of Fe s and z while in $Fe(CO)_3$ there is added some Fe z^2 contribution and rather important delocalization to the carbonyls. Consequently, it is higher in energy in $[Fe(Cp)]^-$. On the other hand, the e set is more heavily delocalized to the ligands in $[Fe(Cp)]^-$ than in $Fe(CO)_3$, and lies slightly higher in energy. A detailed overlap analysis of the bonding properties of these two fragments shows that $[Fe(Cp)]^-$ is a better σ-acceptor, but that $Fe(CO)_3$ is better at π-bonding in interaction with another fragment [8]. These features led us to conclude that in the
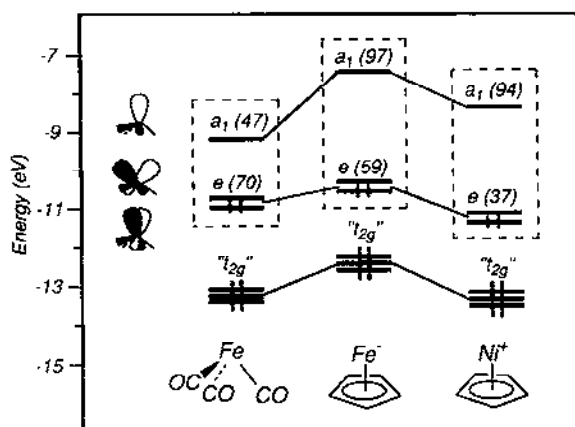

Fig. 4. Comparison of the frontier orbital of $Fe(CO)_3$, $[Fe(Cp)]^-$ and $[Ni(Cp)]^+$. The numbers in parentheses indicate the percentage metal character.

7-SEP *nido* $[Fe_3(Cp)_2(CO)_3(\mu_3\text{-}(II)\text{-}C_2H_2)]^{4-}$ model, the alkyne is more strongly bound to the metallic triangle if it is π-bonded to the $Fe(CO)_3$ moiety and σ-bonded to the $Fe(Cp)$ units [26]. However, we must be aware that the differences between these two isolobal entities can be seen as minor perturbations superimposed on basically similar patterns, explaining the tiny energy difference between *nido* isomers (14) and (15). Undoubtedly, the orientation of the alkyne ligand in these *nido* species is very sensitive to the bonding capabilities of the different fragments. As quoted by Pétillon and colleagues, small changes of the coordination sphere of the $[Fe_3(Cp)_2(CO)_3C_2]$ framework may stabilize the calculated unfavored model (15) [49]. Particularly, the influence of the substituents borne by the C_2 vector may be important. We know examples of trimetallic–alkyne complexes in which the nature of the termini of the alkyne ligand is crucial in determining the M_3C_2 skeletal arrangement (vide supra) [28,50,51]. Calculations are lacking on the influence of the substituents on the alkyne in the trimetallic–alkyne clusters.

14   **15**
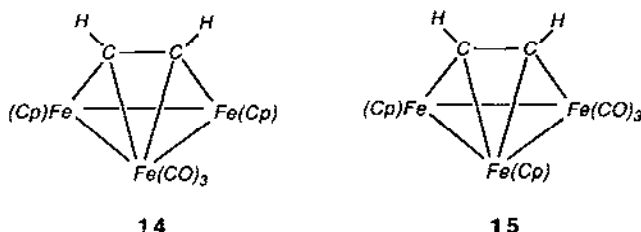
Analogous results have been reported by Dickson et al. [52], who investigated the fluxional properties of the cationic species $[Rh_3(Cp)_2(CO)(CN\text{-}t\text{-}Bu)_3(\mu_3\text{-}(II)\text{-}C_2(CF_3)_2)]^+$ [52]. The symmetrical isomer (16) with the hexafluorobut-2-yne ligand π-attached to the $Rh(CN\text{-}t\text{-}Bu)_3$ fragment is observed in the solid state. However, in solution the two isomers, symmetrical (16) and asymmetrical (17), coexist, with the form (17) being predominant (10 (16) : 1 (17) in $CDCl_3$). Clearly, the stabilities of the different isomers must be very similar. The preferred orientation of the alkyne ligand seems to be extremely sensitive to a range of extraneous parameters, such as, for instance, the crystal packing forces or the weak coordination of solvent molecules.

16   **17**
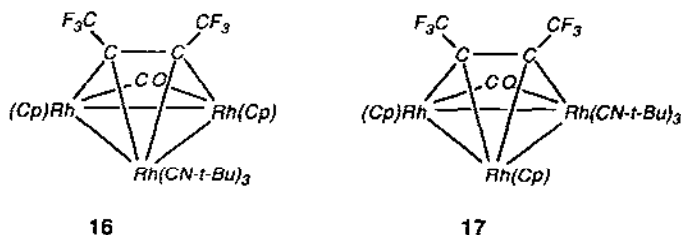
3.3. Nonclassical trimetallic–alkyne clusters

In addition to the *nido* and *closo* arrangements encountered for the M_3C_2 compounds, a third one, unexpected according to the PSEP rules and called basket-like,

has been reported by Adams [50] and Deeming [51] with $Os_3(CO)_9(\mu\text{-}H)_2(\mu_3\text{-}HC_2NEt_2)$ (**18**). Such a compound consists of a triangular osmium array with a triply bridging aminoethyne ligand lying perpendicular to a metal–metal edge. However, this μ_3-($\perp$) bonding mode of the alkyne differs significantly from that in the 6-SEP *closo* M_3C_2 complexes. In the latter examples both ethyne carbon atoms are bonded to the perpendicular vector of the cluster (see (**6**)). In (**18**) the ligand is shifted away from that metal–metal edge so much so that the carbon atom bearing the amino group is linked to only one metal atom. X-ray and NMR measurements support the formulation of a dimetallamethyl(diethylamino) carbene for the C_2 ligand, and indicate that complex (**18**) can be considered an electron-precise molecule [50,51]. Appropriate mesomeric Lewis formulae are given in (**19**) [51].
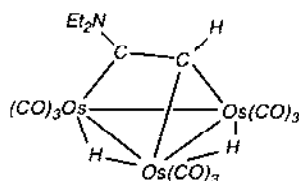
18
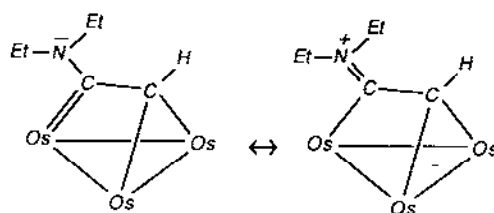
19

This rather scarce and unusual arrangement of the M_3C_2 core of compound (**18**), which possesses 54 CVEs (48 "metallic" electrons) or 7 SEPs, can be regarded as a skeletal isomer of the *nido* form (**7**). This example illustrates how the particular nature of the substituents borne by the C_2 ethyne ligand can produce some geometric distortion of the M_3C_2 core and lead to nonclassical trimetallic alkyne compounds [53].

We have analyzed and compared in detail the bonding of the basket-like compound (**18**) with that of the alternative *closo* and *nido* forms [28]. Different M_3C_2 cluster models were used in order to demonstrate that the unusual coordination of the aminoacetylene ligand to the trimetallic array was mainly due the π-donor effect of the amino substituent on the alkynyl grouping.

As expected, calculations performed on the *closo* model $Os_3(CO)_9(\mu_3\text{-}C_2H_2)$ of C_s symmetry indicate a large HOMO–LUMO gap for the count of 52 CVEs or 6 SEPs, in agreement with the PSEP rules (see above). The LUMO of the *closo* geometry becomes less antibonding and consequently is energetically stabilized when the alkyne ligand C_2H_2 is slipped away from the spanned osmium–osmium bond towards the other osmium atom. This slipping motion is sufficient to move from the *closo*

geometry to the basket-like structure. When the basket-like structure is obtained, the energy of this MO becomes close to that of a set of occupied bonding/nonbonding skeletal MOs. Its occupation secures a large HOMO–LUMO gap for a total count of 54 CVEs or 7 SEPs, in agreement with the observed electron count of compound (18) [28].

The most important question concerns the stability of the 54-electron basket-like complex with respect to its isoelectronic *nido* isomer, which is expected according to the PSEP electron-counting procedure. Extended Hückel calculations on the 54-electron model $[Os_3(CO)_9(C_2H_2)]^{2-}$ give a preference for the *nido* complex [28]. On the other hand, when the hydrogen atom borne by one carbon atom of the ethyne ligand is replaced by an electron-donating NH_2 amino group, the basket-like arrangement becomes slightly preferred over the *nido* one, in agreement with the experiments. It turns out that the π-donor NH_2 group somewhat modifies the shape and the energy of the frontier orbitals of the acetylenic entity, particularly the set of π orbitals which are pushed up in energy. This appears to be a result of interactions of the lone pair of electrons on the nitrogen atom with the alkyne carbon atom to which it is bonded [28]. Consequently, although the MO diagrams for the substituted and non-substituted basket-like structures are strikingly comparable, a difference is noticed in the LUMO region. A better energy match between some metallic and acetylenic FMOs in the amino-substituted complex leads to a greater destabilization of antibonding MOs and a greater stabilization of their corresponding bonding ones. This gives rise to a larger HOMO–LUMO gap comparable to that obtained for the substituted *nido* model. Such a large HOMO–LUMO gap is probably one of the reasons explaining the resistance of the basket-like arrangement to a further deformation toward the *nido* geometry.

Several trimetallic alkyne complexes containing electron-donating substituents on the alkyne moiety have been structurally characterized. Some are listed in Table 2. A glance at the $d[M-C(R')]/d[M-C(R)]$ ratio (r) corresponding to $d[M(3)-C(1)]/d[M(3)-C(2)]$ in (20), indicates that the deviation from the μ_3-(II) parallel mode (*nido* geometry, $r=1$) toward the "slipped" μ_3-($\perp$) perpendicular mode (basket-like geometry, $r \approx 1.3$) increases with the donor capabilities of the alkyne R' substituent (OEt < NMe$_2$ < NEt$_2$) [57]. In fact, only a small "windshield wiper" motion of approx. 30° is sufficient to move from one geometry to the other (see (20)). Moreover, the basket-like geometry is proposed as an intermediate arrangement by McGlinchey and colleagues for the isomerization mechanism of the *nido* M_3C_2 compounds (see (11b,d)) [33].

The extended Hückel total energy change as function of the twisting of the alkyne ligand from *nido* geometry to basket geometry, for the non-substituted and the substituted trimetallic alkyne model $[Os_3(CO)_9(HC_2R)]^{2-}$ (R = H/NH$_2$) has been computed [28]. As expected, the non-substituted model favors the *nido* arrangement. On the other hand, a very soft potential energy profile is computed for the *nido*/basket-like interconversion of the substituted complex with a shallow and broad minimum for the basket-like geometry. The electron-donating properties of the amino substituent are strong enough to rotate the aminoalkyne ligand from a parallel μ_3-(II) to a perpendicular "slipped" μ_3-($\perp$) orientation. Throughout the

Table 2
Structurally characterized trimetallic substituted alkyne complexes $M_3(CO)_9(\mu\text{-H})_2(\mu_3\text{-RC}_2R')$

Compound	$d(M-C(R))^a$	$d(M-C(R'))$	r^b	$d(C-X)^c$	Ref.
$Os_3(CO)_6(H)_2(C_6H_4)$	2.31(3)	2.37(3)	1.026		
	2.33(4)	2.46(3)	1.055		54
$Os_3(CO)_6(H)_2(HC_2OEt)$	2.32(4)	2.45(5)	1.056	1.58(5)	55
$Ru_3(CO)_9(H)_2(MeC_2OMe)$	2.221(5)	2.391(5)	1.077	1.353(6)	56
$Os_3(CO)_9(H)_2(C_4H_2S)$	2.23(2)	2.46(2)	1.103	1.72(2)	
	2.31(2)	2.43(2)	1.052	1.65(2)	57
$Os_3(CO)_9(H)_2(C_4H_2NMe)$	2.24(2)	2.56(2)	1.143	1.38(3)	
	2.24(2)	2.50(2)	1.116	1.36(3)	57
$Os_3(CO)_9(H)_2(MeC_2NMe_2)$	2.25(2)	2.62(2)	1.164	1.40(2)	58
$Os_3(CO)_6(H)_2(HC_2NEt_2)$	2.14(2)	2.80(2)	1.308	1.33(2)	50
	2.144(15)	2.807	1.309	1.307(18)	51
$Ru_3(CO)_9(H)_2(HC_2N\text{-}i\text{-}Pr_2)$	2.146(8)	na^d		1.330(9)	59

^{a} Distances are given in Å; $^b r = d(M-C(R'))/d(M-C(R))$; ^{c} X, electron-donating heteroatom of the substituent R' of the alkyne ligand; ^{d} na, not available.
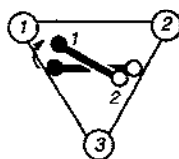
20

"windshield wiper rotation" process HOMO–LUMO gap values over 1 eV were computed, which are reasonable criteria for complex stability. These results are in agreement with the different characterized compounds gathered in Table 2, which adopt a range of structures between *nido* and basket-like [57]. Note that being close in energy to each other, an interconversion between the basket-like and *nido* structures cannot be ruled out in solution. According to Deeming and colleagues, this is observed for $Os_3(CO)_9(H)_2(\mu_3\text{-HC}_2OEt)$ but not for $Os_3(CO)_9(H)_2(\mu_3\text{-HC}_2NEt_2)$ [51,55]. If such an interconversion was possible in the case of M_3-(ynamine) compounds, it should be accompanied by the change of a short, nearly double, C–N bond in the basket-like geometry (see (19)) into a single C–N bond in the *nido* one (see (21)). The hexaruthenium complex $Ru_6(CO)_{13}(\mu\text{-MeC}_2NMe_2)(\mu_3\text{-MeC}_2NMe_2)(\mu_4\text{-S})_2$ (22) provides a nice example for this statement (the asymmetric μ-bridging ynamine ligand is not shown for clarity) [60]. Such a cluster, which can be described as a Ru_6S_2 monocapped pentagonal bipyramid, contains one ynamine ligand linked in an asymmetrical edge bridging mode [53] and the other as a triple bridge, adopting the classical μ_3-(⊥) alkyne coordination. The nitrogen atom is planar and the C–N bond length is short (1.32 Å) in the former. On the other hand, the nitrogen atom is somewhat pyramidalized and the C–N bond length is rather long (1.40 Å) in the latter, indicating that the lone pair donation from the

nitrogen atom to the carbon atom to which it is tethered is considerably less than that in other aminoacetylene compounds [60]. Note also that for a given family of substituted alkyne–trimetallic clusters, the bond distance between the electron-donating heteroatom X (X = N, O, S) and the adjacent carbon atom gradually lengthens as the C_2 ligand deviates from the idealized "slipped" perpendicular coordination mode (see Table 2).

21   **22**
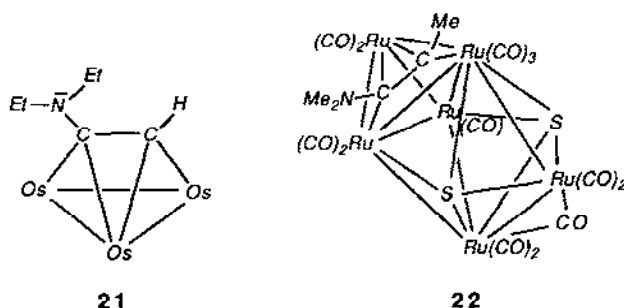
The formal addition of two electrons to basket-like M_3-(ynamine) compounds leads to an opening up of a metal–metal bond, and leaves the ynamine ligand asymmetrically bonded to the three metal atoms. Here again, the unexpected geometry adopted by the 8-SEP M_3-(ynamine) clusters, such as $Os_3(CO)_9(\mu_3$-S)$(\mu_3$-MeC$_2$NMe$_2$) (**23**), can be attributed in part to strong interactions of the nitrogen lone pair of electrons with the adjacent carbon atom of the C_2 ligand [61]. A classical *nido* arrangement of a pentagonal M_3SC_2 pyramid is observed if the C_2 unit bears innocent substituents, as in the 8-SEP compound $Ru_3(CO)_9(\mu_3$-S)$(\mu_3$-HC$_2$Ph) (**24**) [62].

23   **24**
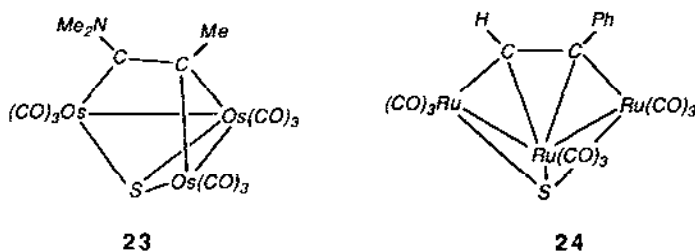
3.4. Alkyne (or alkyne-like) scission on a trimetallic framework

The scission of alkyne ligands taking place on trimetallic frameworks is of considerable interest and is now rather well documented. A special case is the alkyne cleavage yielding two alkylidyne fragments bonded to the metal triangle [63–74]. According to the Wade–Mingos rules, the M_3C_2 core of 6-SEP bis(alkylidyne) compounds such as $Co_3(Cp)_3(\mu_3$-CSiMe$_3)(\mu_3$-CC$_2$SiMe$_3$) (**25**) [66] represents an alternative skeletal isomeric form of the one encountered in 6-SEP alkyne trimetallic species (**6**). We simply formally obtain the former by rupture of the C–C bond in the latter. Direct

experimental evidence for the conversion of 6-SEP *closo* alkyne complexes to 6-SEP *closo* bis(carbyne) compounds is scarce [71,72]. Interconversion seems rather to occur between 7-SEP *nido* alkyne clusters and 6-SEP *closo* bis(carbyne) species with loss of CO [67,69,70,74]. It is generally admitted that the different interconversions are intramolecular, but they are mechanistically rather ill-defined and the necessity or not of an additional two-electron ligand in these trinuclear species as a requirement for alkyne cleavage is still controversial though having been amply discussed [67,71].
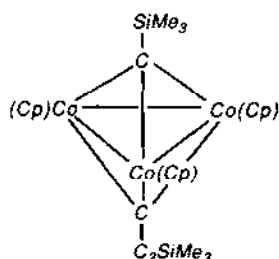
25

Shapley, Hoffmann and coworkers have tentatively demonstrated, on the basis of experimental and theoretical studies on $Rh_3(Cp)_3(CO)(C_2Ph_2)$, that the presence of the carbonyl ligand triggers the alkyne rupture by reducing the energy barrier to alkyne cleavage and favors then the formation of the 6-SEP bis(carbyne) trimetallic species [67]. The reaction pathway they proposed is given in (**26**). Surprisingly, the first step transforms the 7-SEP *nido* $M_3(\mu_3\text{-}(\text{II})\text{-}C_2)$ starting species (**26a**) into a 7-SEP *closo* $M_3(\mu_3\text{-}(\perp)\text{-}C_2)$ structure (**26b**), which is generally unstable for such an
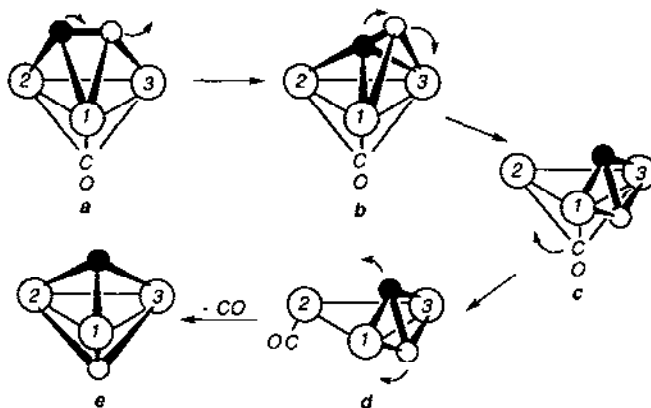
26

electron count (see above) [23–28]. According to the authors, no evidence for a 6-SEP *closo* compound $Co_3(Cp)_3(\mu_3\text{-}(\perp)\text{-}C_2Ph_2)$ was found experimentally. The next step is the motion of the alkyne ligand to an edge-bridging position, accompanied by a shift of the extra CO ligand from triply-bridging to terminal in order to satisfy

electronically the metal center not involved in the alkyne edge-bridging (26c,d). Finally, the loss of the carbonyl concerted with the dissociation of the alkyne leads to the final 6-SEP $M_3Cp_3(\mu_3$-CR$)_2$ product (26e).

The presence of the CO ligand all along the interconversion process until the alkyne is cleaved is contradictory somewhat to studies undertaken some time ago by Vollhardt et al. or more recently by Pétillon et al. on bis(alkylidyne)–tricobalt complexes [71,74], and Vahrenkamp and colleagues on bis(nitrene)–triiron clusters [75,76]. These authors have demonstrated that an additional ligand in the cluster ligand sphere is not a prerequisite for bis(carbyne) or bis(nitrene) cluster generation.

As part of their investigation on the activation of multiply C–C–, C–N– and N–N–bonded substrates on metallic cluster frameworks, Wucherer and Vahrenkamp have shown that thermolysis of the azoalkane–triiron compound $Fe_3(CO)_9(\mu_3$-(II)-N_2Et_2) (27) has resulted in N–N scission and formation of the bis(nitrene) cluster $Fe_3(CO)_9(\mu_3$-NEt$)_2$ (28). Kinetic experiments suggest that the transformation of (27) into (28) is intramolecular and proceeds first by elimination, and then readdition of a CO ligand, since both have the same composition [75,76].

27   28
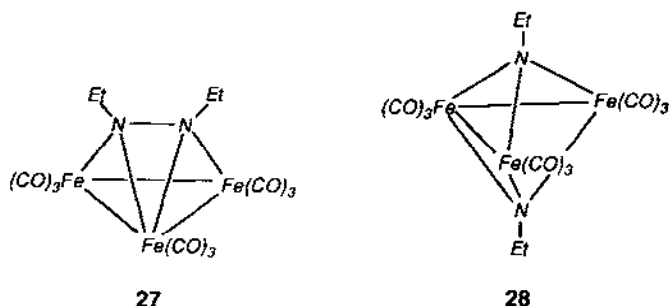
Indeed, these two 5-vertex M_3N_2 compounds can be described as *nido* square-pyramidal species in agreement with their 54 CVEs or 7 SEPs. Here again, the respective stability of these skeletal isomers and the possibility of their interconversion lie beyond the capability of the PSEP theory. Using EHMO calculations, we have theoretically explored the potential energy surface of the (27)→(28) transformation [76]. Several possible pathways were considered. Only that in agreement with the kinetic results, involving CO loss and capture, is recalled here in (29).

The first step of the reaction described in (29) is the slipping of the alkyne over the trimetallic array accompanied with the loss of CO, leading to the formation of the 6-SEP *closo*-trigonal-bipyramidal thermodynamically stable intermediate $Fe_3(CO)_8(\mu_3$-($\perp$)-N_2R_2) (29b), analog to $Fe_3(CO)_9(\mu_3$-($\perp$)-C_2Ph_2) (6). Calculations have indicated that (29b) can easily rearrange into a more stable isomeric form, the 6-SEP bis(nitrene) species $Fe_3(CO)_8(\mu_3$-NR$)_2$ (29d). This occurs with the cleavage of the N–N bond and the rocking motion of one NR group to the other side of the iron triangle via the 6-SEP bridged *nido*-tetrahedral intermediate $Fe_3(CO)_8(\mu_3$-NR)(μ-NR) (29c). In the final step a CO ligand is picked up and one metal–metal bond is broken, giving the final product (28). These results lead us to think that the (27)→(29d) transformation is probably the least-motion pathway in

29
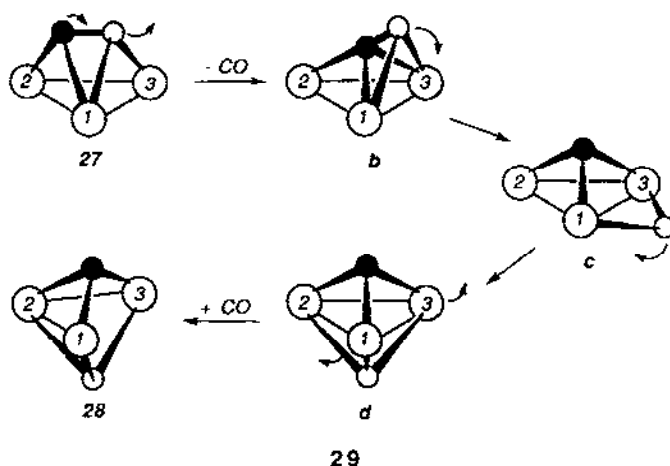
the reaction process between the 7-SEP *nido* alkyne–trimetallic and 6-SEP biscarbyne–trimetallic systems mentioned above. It appears also from this study that among different key features proposed earlier to prompt alkyne (or alkyne-like) cleavage, such as the induction of electronic unsaturation of the trimetallic array [77] or the particular electron-donating nature of the alkyne substituents [70,74], the one concerning the presence of a spectator two-electron ligand such as CO in the cluster ligand sphere until the C–C dissociates is not required.

4. Alkyne (or alkyne-like) complexes of tetrametallic clusters

4.1. Closo-octahedral heterotetrametallic alkyne complexes

Alkyne coordination to tetrametallic clusters gives almost exclusively 7-SEP *closo*-octahedral M_4C_2 compounds, in which the C_2 ligand is σ-bonded to the hinge and π-bonded to the apices of the metallic butterfly framework [18], e.g., $Fe_4(CO)_{12}(\mu_4\text{-}\eta^2\text{-}C_2Me_2)$ (30) [78]. In agreement with the PSEP rules EH calculations show that such a geometry gives rise to a large HOMO–LUMO gap only for the expected count of 7 SEPs (or 66 CVEs) [79–81]. Indeed, compound (30) can be formally seen as a cluster expansion of the 7-SEP *nido*-octahedral $M_3(\mu_3\text{-}(II)\text{-}C_2)$ complexes described above, upon addition of a zero-skeletal-electron $[Fe(CO)_3]^{2+}$ fragment to the vacant vertex (31). This cluster expansion illustrates how the PSEP theory can facilitate structural relationships in cluster chemistry.

Among the metallic-butterfly-alkyne complexes which have been characterized, a limited number of mixed-metal examples have been reported (see Table 3). The PSEP electron-counting rules do not provide insight into the "hinge-apex" metal isomerism encountered in these heterotetrametallic–alkyne complexes. As in the case of the heterotrimetallic–alkyne species mentioned above (see Section 3.1), only one skeletal isomer is generally observed in the solid state with often the less electronegative

30

31
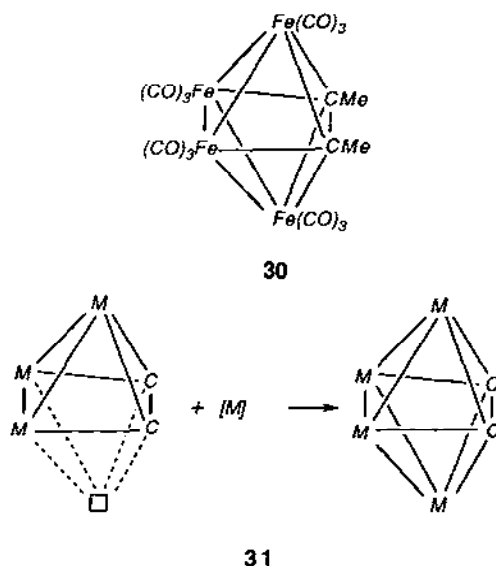
metal atoms occupying the wing-tip sites. This is in accord with FH calculations performed by Osella and coworkers on $Co_4(CO)_{10}(\mu_4-C_2H_2)$ which indicate that the Co wing-tip atoms are more positively charged than the hinge atoms [80]. However, examples of skeletal isomerism in the solid state have been noticed such as for $FeRu_3(CO)_{12}(\mu_4-C_2Ph_2)$, (32) and (33). In solution, isomer (33) interconverts to isomer (32) upon heating, indicating that (32) is slightly more thermodynamically stable [86]. This suggests a quite small difference energy between the two structures.

The same phenomenon, i.e. one single structural isomer, is usually observed in 7-SEP *arachno* mixed-metal butterfly complexes containing an exposed main group element [98]. FH calculations have shown that the MO diagrams of the mixed-metal butterfly carbide cluster $[Fe_3Rh(CO)_{12}(\mu_4-C)]^-$ (34) and $[Fe_3Mn(CO)_{13}(\mu_4-C)]^-$ (35) for instance, are markedly different from that of their homometallic homologue $[Fe_4(CO)_{12}(\mu_4-C)]^{2-}$, particularly in the HOMO region where are found the pertinent orbitals responsible for the M–M bonding [99]. The HOMO is now predominantly localized on the wing-tip Fe atoms and the most electropositive hinge atom, i.e. Fe and Mn in the Fe_3Rh and Fe_3Mn clusters, respectively. Changes are ascribed to the lowering of symmetry of the butterfly core from C_{2v} to C_s and the difference of the energies of the FMOs of the constituting metallic fragments. This should imply some change in their reactivity compared to that of homometallic butterfly clusters. However, no conclusions were drawn to rationalize the preference of the heterometal atom in the occupation of the hinge site of the butterfly framework. Consequently, these calculations are not very helpful to tackle the "hinge-apex" isomerism in isoelectronic *closo* heterometallic-butterfly-alkyne complexes. Theoretical studies would be desirable in order to understand the intimate role of the nature of the metal atoms, the nature of the terminus ligands of the

Table 3

Selected X-ray structurally characterized *closo*-octahedral heterotetrametallic-alkyne compounds $M_4L_n(\mu_4\text{-}C_2R_2)$

Compound	Apical vertex[a]	$d(C-C)$ (Å)	Ref.
$Fe_3Co(Cp)(CO)_9(C_2F_2)$	Co/Fe	1.450(2)/1.43(2)	82
$FeCo_2Rh(Cp)(CO)_7(HC_2Me)$	Fe/Co	1.412(10)/1.428(10)	83
	Co/Co	1.404(10)	
$FeCo_3(CO)_9(PhC_2(H)Ph)(C_2Ph_2)$	Fe/Co	1.41(2)	84
$Fe_3Ni(Cp)(CO)_7(PPh_2)(HC_2\text{-}i\text{-}Pr)$	Fe/Fe	1.436(16)	85
$FeRu_3(CO)_{12}(C_2Ph_2)$	Fe/Ru	1.460(3)	
	Ru/Ru	1.458(4)	86
$FeRu_3(CO)_{12}(C_2Me_2)$	Fe/Ru	1.46(2)	
	Ru/Ru	1.46(2)	86
$Fe_3Rh(Cp)(CO)_9(C_2Me_2)$	Fe/Fe	1.448(13)	87
$Co_2Mo_2(Cp)_2(CO)_8(C_2Me_2)$	Mo/Mo	1.47(1)	88
$Co_2Mo_2(Cp)_2(CO)_4(S)_2(C_2Me_2)$	Co/Co	1.455(7)	89
$Co_2MoRuRh(Cp)_2(CO)_7(C_2Me_2)$	Co/Mo	1.414(9)	
	Co/Ru	1.400(15)	86
$Co_3Ru(CO)_9(PPh_2)(HC_2Bu^t)$	Co/Co	1.424(5)	90
$[Co_3Ru(CO)_{10}(C_2Ph_2)]^-$	Co/Co	1.34(1)/1.43	37
$Co_2Ru_2(CO)_{11}(C_2Ph_2)$	Co/Co	1.432(5)	91
$Co_2Rh_2(CO)_{10}(C_2(C_6F_5)_2)$	Co/Co	1.369(23)	92
$Co_2Rh_2(CO)_9(PPh_3)(HC_2\text{-}n\text{-}Bu)$	Co/Co	1.43(1)	93
$Co_3Rh_2(CO)_{10}(C_2Ph_2)$	Co/Co	1.42(1)	94
$Ni_2Re_2(Cp)_2(CO)_6(PhC_2C(H)C(H)Ph)$	Re/Re	1.48(2)	95
$Mo_2Re_2(Cp)_2(CO)_{10}(PhC_2H)$	Mo/Re	1.47(2)	96
$RuOs_3(C_6H_6)(CO)_9(C_2Me_2)$	Ru/Os	1.48(3)	97

[a] Metal atoms occupying the apical vertices of the *closo*-octahedral M_4C_2 core.
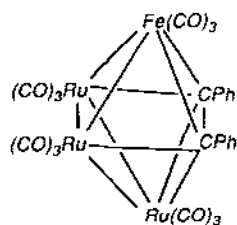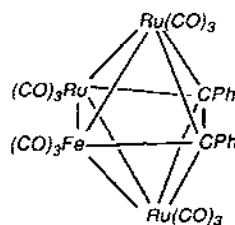
32   33

alkyne moiety and/or the surrounding ligands (CO, PR_3, Cp, C_6H_6...) in the choice of the site (hinge or apex) occupied by the different metal atoms in these systems.

4.2. Other coordination modes of alkyne (or alkyne-like) ligands in tetrametallic butterfly clusters

Though the *closo*-octahedral arrangement is the most common one encountered for M_4C_2 clusters, alternative geometries are theoretically possible, some of which
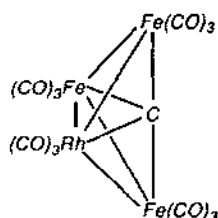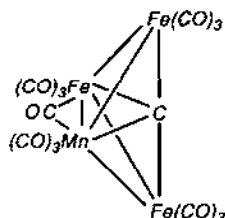
34   **35**

have been observed. According to the PSEP rules and the capping principle (see Section 2), another way to expand the square-pyramidal $M_3(\mu_3\text{-}(II)\text{-}C_2)$ compounds would be to cap the triangular metallic face by a formally zero-skeletal-electron ML_n fragment, leading to a 7-SEP capped *nido*-square-pyramidal $M_4(\mu_3\text{-}(II)\text{-}C_2)$ complex as observed for $WOs_3(Cp)(CO)_{10}(H)(\mu_3\text{-}(II)\text{-}C_2Tol_2)$ (**36**) [100]. Capping a triangular M_2C face also affords a 7-SEP capped *nido* square-pyramidal $M_4(\mu_4\text{-}C_2)$ complex. One example of such an arrangement has been observed, not with an alkyne ligand, but with the isoelectronic nitrile analogue, namely $Fe_4(CO)_{12}(\mu_4\text{-}NCPh)$ (**37**) [101].
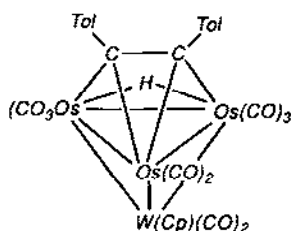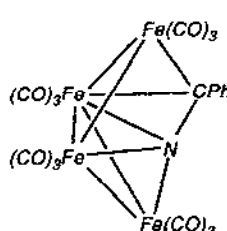
36   **37**

Structural arrangements (**30**) and (**37**) can in turn be viewed as alternative skeletal isomeric geometries for 7-SEP (or 66-CVE) M_4E_2 species (E = N or CR). This prompted us to study their electronic structure, particularly the various factors favoring their respective stability and the possibility of their interconversion with the aid of EH calculations [81]. Using the isolobal analogy between different E_2 ligands (C_2R_2, NCR, $[N_2R_2]^{2+}$ or N_2) [81], 7-SEP models $Fe_4(CO)_{12}(\mu_4\text{-}N_2)$ were used for the calculations. Among the different interconversion pathways which were envisaged, calculations indicated that the one described in (**38**) is the most energetically favorable. A simple displacement of the N_2 ligand corresponding roughly to a combined rotation and translation motion in the groove of the Fe_4 butterfly framework, accompanied by a small variation of the butterfly angle (from $\sim 100°$ to $\sim 135°$), affords progressively the transformation of the octahedral structure (**38a**) into the capped-square-pyramidal arrangement (**38c**). Our calculations have shown that both (**38a**) and (**38c**) are quite comparable electronically. The fact that (**38c**) has not been reported yet, with alkyne ligands, may be merely due to steric hindrance around the four-connected N atom. No symmetry element is retained throughout the interconversion process and therefore the reaction is formally symmetry-allowed.

During the interconversion, two M–E contacts are broken while one is created, reflecting the delocalized bonding picture in these types of isoelectronic cluster. Consequently, a HOMO/LUMO avoided crossing occurs, which is responsible for the computed energy barrier of ~ 0.7 eV. Such a qualitative value suggests strongly that structure-types (38a) and (38c) can theoretically interconvert in solution. These results also suggest that despite the fact that the four-connected main group atom is somewhat sterically hindered in (38c), the octahedron↔capped-square-pyramid polyhedral rearrangement proposed in (38) should constitute the first step of the "alkyne" isomerism reported for $FeRu_3(CO)_{12}(\mu_4\text{-}PhC_2Me)$ for instance [86]. Note also that such an interconversion process constitutes a model of a possible reaction path for the interconversion of the 7-SEP hexanuclear species $[Os_6(CO)_{18}]^{2-}$ (4) and $Os_6(CO)_{18}H_2$, which adopt an arrangement identical to that of the models (38a) and (38c), respectively [9].

38
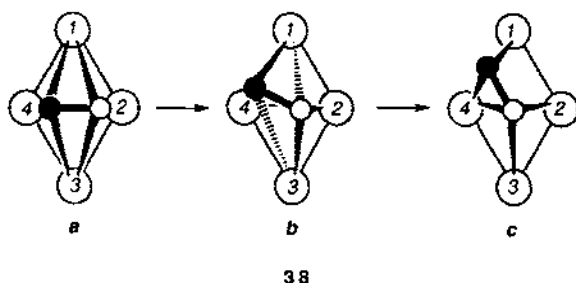
With two electrons more, i.e. 8 SEPs or 68 CVEs, *closo*-octahedral $M_4(\mu_4\text{-}E_2)$ such as (30) are expected to distort towards more open structures obtained by rupture of either M–M, M–E or E–E bonds. The formal cleavage of the hinge metal–metal bond leads to the formation of the *nido*-pentagonal-bipyramidal arrangement, exemplified by $Fe_2Ni_2(Cp)_2(CO)_6(\mu_4\text{-}C_2Ph_2)$ (39)

39
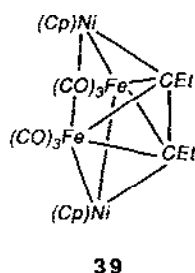
[102], which with a count of 8 SEPs obeys the Wade–Mingos rules. The formal dissociation of the E–E bond can also afford the *nido* pentagonal-bipyramidal structure as reported for the 8-SEP compound $Ru_4(CO)_{10}(C_2Ph_2)(\mu_4\text{-}NPh)_2$ (40) [103], consistent with the PSEP procedure. On the other hand, the structural arrangement of the 8-SEP electron-precise complex $Ru_4(CO)_{12}(\mu_4\text{-}N_2Et_2)$ (41), which can be derived from the octahedron (30) by breaking two M–E bonds, is rather unexpected within the PSEP framework [78,104].

40   **41**
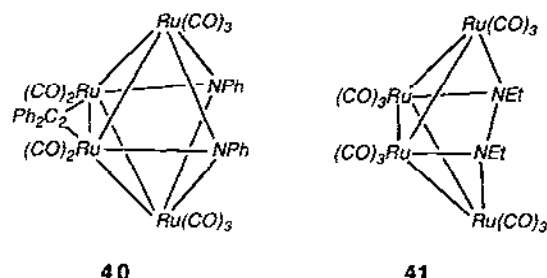
Structural arrangements (40) and (41) can be considered as being alternative skeletal isomeric geometries for 8-SEP M_4E_2 species. As for the 7-SEP geometries (30) and (37), we have theoretically investigated the interconversion between (40) and (41) using 8-SEP models $[Fe_4(CO)_{12}N_2]^{2-}$ (see (42)) [81]. The least-motion pathway for the (42a)→(42b) transformation involving a rotation of the N_2 vector simultaneously accompanied by the N–N bond breaking was computed to be symmetry-forbidden. Consequently, this rules out the interconversion of (42a) into one of its topological stereoisomers (42a') via intermediate (42b). If a fluxional behavior of compounds of type (42a) were observed, it should occur via other routes. The octahedral structure of type (30) as an intermediate structure must also be discarded, being very unstable for the count of 8 SEPs as predicted by the Wade–Mingos rules. Moreover, the (42a)→(30) pathway is also symmetry-forbidden. In fact, the easiest symmetry-allowed reaction process that we found to interconvert 42a into one of its topological stereoisomers is the hypothetical (42a)→(42a'') skeletal rearrangement. It corresponds to a rotation of the N–N vector in such a way that it becomes parallel to the wing-tip vector in the basket-like intermediate structure (42c). Note that such a quite open structural geometry has been reported for the 10-SEP tricyclic polyphos-

4 2
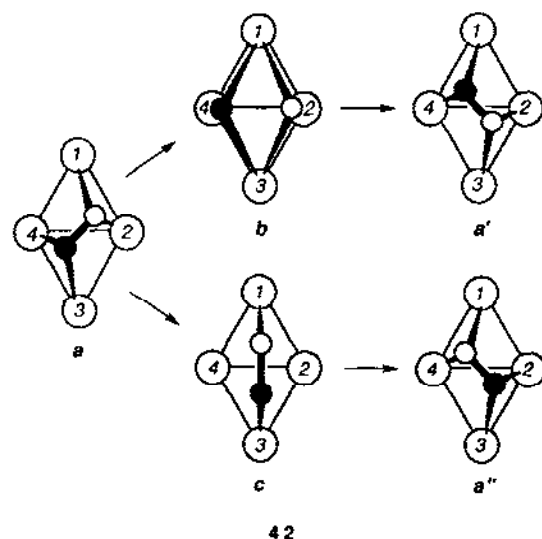
phane compound $P_6(C_5Me_5)_2$ [105]. With a count of 8 SEPs, model (42c) is Jahn-Teller unstable with two nonbonding MOs vacant, and thus must be considered as a transition state rather than an intermediate structure. A flattening of the metal butterfly array accompanied with the rupture of hinge metal–metal bond would afford the stable 8-SEP arrangement analogous to that of (39). But again, this would involve forbidden HOMO–LUMO crossings.

The different fluxional processes illustrated here for tri- and tetrametallic–alkyne (or alkyne-like) complexes on the basis of symmetry arguments and EH calculations reveal that skeletal rearrangement processes must avoid intermediate structures that are not suited for the right electron count, i.e. structures where there is an occupied high-lying antibonding MO. This must be accompanied by a minimum change of the cluster cohesive energy [81,106].

5. Breakdown of the PSEP rules: examples in mixed transition metal–main group clusters

The large HOMO–LUMO gap which is generally computed between the bonding/ nonbonding and antibonding MOs for main group clusters and their transition metal carbonyl analogues explains partly the success of the PSEP theory. Few deviations from these rules have been noticed, and they have been rationalized on the basis of symmetry arguments in the case of deltahedron boranes [1e].

Very few deviations are observed for transition metal carbonyl clusters made of conical fragments [1e]. On the other hand, since the electron-counting rules veil the differing electronic and steric demands of main group and metallic fragments, exceptions are found in compounds with heteronuclear cores. We focus here on particular mixed main group–transition metal clusters where the bonding requirements (electronegativity and overlap) of the different types of fragments constituting the cluster are quite dissimilar.

5.1. Mixed transition metal–main group octahedral clusters

The octahedral $M_4(\mu_4\text{-}CR)_2$ core arrangement analogous to that of $Ru_4(CO)_{12}(\mu_4\text{-}Bi)_2$ (1) [2] in which the metal atoms define a square, constitutes a possible structural isomer of the M_4-alkyne compound (30). Although alkyne C–C cleavage on tetranuclear metallic complexes has been observed [74,100,107], no example of bis(alkylidyne) $M_4(\mu_4\text{-}CR)_2$ complexes has been reported yet. Only one example of such an arrangement has been observed so far with main group atoms of the second row of the periodic table, namely the 7-SEP compound $Fe_4(CO)_{11}(\mu_4\text{-}NEt)_2$ (43) [104]. It turns out that this structural geometry is extremely rare for small main group atoms mainly because of geometric factors. However, we have performed EH calculations on $Fe_4(CO)_{12}(\mu_4\text{-}N)_2$ models that have suggested that such species may be capable of existence, possibly with an N–N bond penetrating the iron square [108,109]. The *closo*-octahedral $M_4(\mu_4\text{-}E)_2$ arrangement encountered in (43) is quite common with heavier main group elements, as exemplified by

43
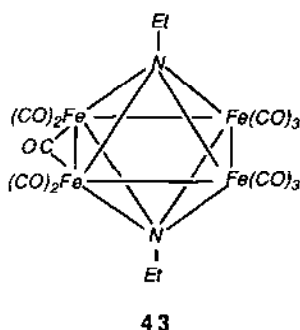
compound **1** [2]. With a count of 7 SEPs $M_4(\mu_4\text{-}E)_2$ complexes possess two electrons less than the number required by the 18-electron rule for a cluster with four metal–metal bonds, but conform to the PSEP theory as their borane and metal analogues $[B_6H_6]^{2-}$ and $[M_6(CO)_{18}]^{2-}$ [110]. Conversely, with two electrons more these species would not obey the PSEP electron-counting procedure, but would satisfy the 18-electron rule. Note the hypervalent character of the capping main group atoms. Surprisingly, most of the $M_4(\mu_4\text{-}E)_2$ clusters which have been characterized so far have 8 SEPs (or 68 CVEs), i.e. two electrons more than the anticipated electron count. Some examples are given in Table 4.

The reasons for the stability of these octahedral 8-SEP "rule-breakers" and their comparison with the 7-SEP analogues has been studied in detail [137–139]. A schematic MO diagram of the *closo*-octahedral model $[Co_4(CO)_{12}(\mu_4\text{-}PH)_2]^{2+}$ is shown on the left-hand side of Fig. 5 [137]. Above a nest of seven occupied skeletal MOs, which corresponds to the anticipated count of 7 SEPs, lies a weakly metal–metal π-antibonding MO ($2a_2$) in the middle of a large energy gap. Such a situation favors the possibility of two electron counts, either 7 SEPs (or 66 CVEs) if the $2a_2$ MO is empty, or 8 SEPs if the $2a_2$ MO is occupied [137]. This MO is exclusively localized on the metallic square. Consequently, its occupation is strongly dependent on the electronegativity of the metal atoms as exemplified by $Fe_4(CO)_{11}(\mu_4\text{-}P\text{-}p\text{-Tol})_2$ [117] and $Co_4(CO)_{10}(\mu_4\text{-}PPh)_2$ [3] possessing 7 and 8 SEPs, respectively. A $2a_2$ level at low energy favors the count of 8 SEPs. Indeed, all $M_4(\mu_4\text{-}E)_2$ clusters which have been structurally characterized are in accord with this statement. Ruthenium affords exclusively 7-SEP systems. With cobalt, only 8-SEP clusters have been observed. Both counts of 7 and 8 SEPs are reported for iron, the electronegativity of which is intermediate between that of Ru and Co [43].

Our theoretical prediction that both 7 and 8-SEP compounds can be observed with the same $M_4(\mu_4\text{-}E)_2$ octahedral framework has been nicely borne out by numerous experimental works [117,119,140]. For instance, Vahrenkamp and colleagues have shown that the 7-SEP species $Fe_4(CO)_{11}(\mu_4\text{-}PR)_2$ easily add reversibly one two-electron ligand L (CO, $P(OMe)_3$, *t*-BuNC) to yield 8-SEP clusters $Fe_4(CO)_{11}L(\mu_4\text{-}PR)_2$ with the same octahedral core arrangement [117]. According to Huttner et al., $Fe_4(CO)_{11}(\mu_4\text{-}P\text{-}t\text{-}Bu)_2$ can be reduced by PhLi to produce radical anions able to react with Et_3OBF_4 to yield the neutral radical cluster $[Fe_4(CO)_{10}(\mu\text{-}$

Table 4
Selected crystallographically characterized electron-rich octahedral compounds $M_4L_n(\mu_4\text{-}E)_2$ and derivatives

Compound	$d(E\cdots E)$ (Å)	Ref.
8-SEP *closo* octahedral complexes		
$Co_4(CO)_{10}(BCo(CO)_3)(BH)$	1.85(4)	109
$Co_4(CO)_{11}(SiMe)_2$	2.726	111
$Co_4(CO)_{10}(GeMe_2)(SiMe)_2$	2.686	111
$Co_4(CO)_{11}(SiCo(CO)_4)_2$	2.817	112
$Co_4(CO)_{11}(GeMe)_2$	2.926	113
$Co_4(CO)_{11}(GeMe)(GeCo(CO)_4)$	2.955	114
$Co_4(CO)_{11}(GeCo(CO)_4)_2$	2.955	115
$Co_3Ni(Cp)(CO)_8(Ge\text{-}t\text{-}Bu)_2$	na[a]	116
$Fe_4(CO)_{11}(P(OMe)_3)(P\text{-}p\text{-}Tol)_2$	2.598(3)	117
$Fe_3Co(CO)_{11}(PPh)_2$	2.566	118
$Fe_3Rh(CO)_9(Cp^*)(PPh)_2$	2.579	119
$Fe_2CoNi(Cp)(CO)_8(PMe)_2$	2.558	120
$Co_4(CO)_{10}(PPh)_2$	2.537(6)	3
$Co_4(CO)_9(PCy_3)(PPh)_2$	2.554(3)	121
$Co_4(CO)_9(CCH_2)(PPh)_2$	2.543(1)	122
$Co_4(CO)_9(CC(OMe)Me)(PPh)_2$	2.534(5)	122
$Co_4(CO)_8(PPh_3)_2(PPh)_2$	2.540(5)	3
$Co_4(CO)_8(P(OMe)_3)_2(PPh)_2$	2.534(2)	123
$Co_4(CO)_8(P(OEt)_3)_2(PPh)_2$	2.541(2)	124
$Co_4(CO)_8(dppm)(PPh)_2$	2.546(4)	125
$Co_4(CO)_8(dppe)(PPh)_2$	2.548(3)	125
$Co_4(CO)_8(dppt)(PPh)_2$	2.509(5)	125
$Co_4(CO)_8(dmpe)(PPh)_2$	2.536(3)/2.530(3)	126
$Co_4(CO)_8(PPh_2H)_2(PPh)_2$	2.518(2)/2.548(2)	127
$Co_4(CO)_6(P(OMe)_3)_4(PPh)_2$	2.554(3)/2.553(3)	123
$Co_4(CO)_{10}(P\text{-}t\text{-}Bu)_2$	2.608(1)	128
$Co_4(CO)_{10}(PCH(SiMe_3)_2)(PCH_2SiMe_3)$	na[a]	129
$Fe_2Co_2(CO)_{11}(S)_2$	na[a]	130
$Co_4(CO)_{10}(S)_2$	2.74(2)	131
$Co_4(Cp)_4(S)_2$	na[a]	132
$Co_4(CO)_{10}(Te)_2$	3.30	3
9-SEP *nido* octahedral complexes		
$Co_4(CO)_3(F_2P)_2NMe)_4(PPh)_2$	2.440(9)	133
$[Co_4(CO)_{11}(Sb)_2]$ [b]	2.911(1)	134
$[Co_4(CO)_{11}(Sb)_2]^2$	2.882(1)	134
$[Co_4(CO)_{11}(Bi)_2]^-$ [b]	3.088(1)	135
$[Co_4(CO)_{11}(Bi)_2]^{2-}$	3.078(3)	134
10-SEP *closo* octahedral complexes		
$Ni_4(Cp)_4(Se)_2$	3.053(1)	136

[a] na, Not available; [b], paramagnetic species with 8.5 SEPs.
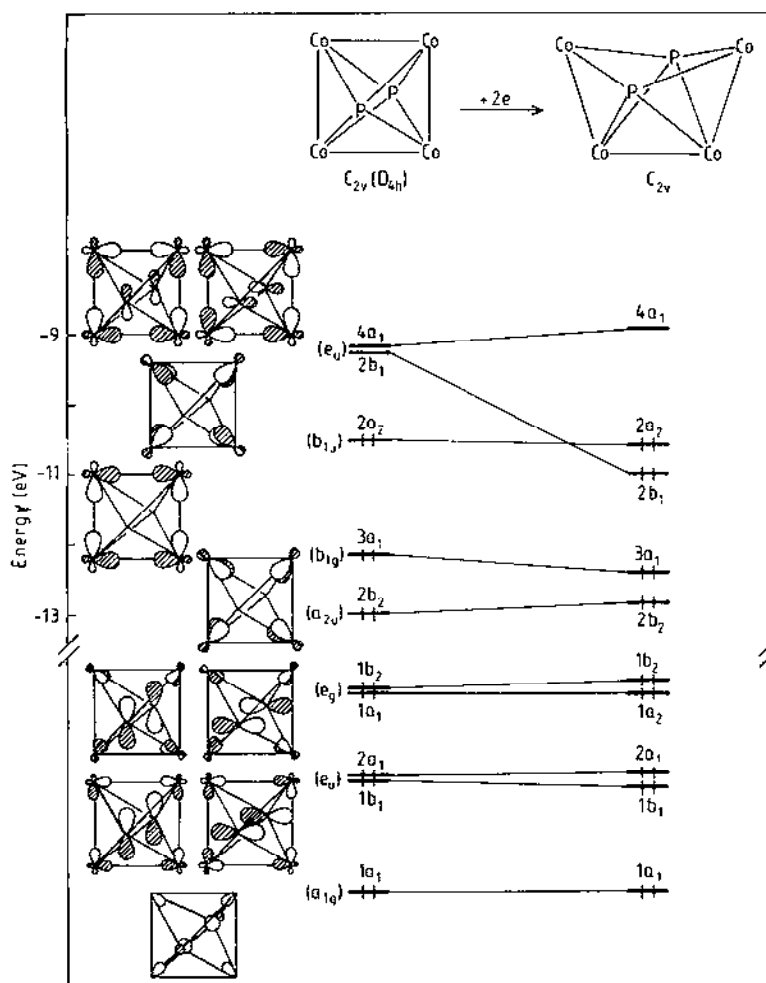
Fig. 5. Skeletal MOs for the model $Co_4(CO)_{12}(\mu_4\text{-PH})_2$ with the *closo* (on the left) and *nido* (on the right) geometry.

$COEt)(\mu_4\text{-P-}t\text{-Bu})_2]^{\pm m}$, in which a carbonyl ligand of the starting material has been alkylated to form a μ-COEt group [140]. These results, which have been further substantiated by electrochemical and EPR investigations, suggest that the additional electron resides in a nonbonding $2a_2$-like MO [140]. Ohst and Kochi have carried out experiments showing that the 7-SEP cluster $Fe_3Rh(CO)_8(Cp^*)(\mu_4\text{-PPh})_2$ reversibly binds a carbonyl group to form the 8-SEP system $Fe_3Rh(CO)_9(Cp^*)(\mu_4\text{-PPh})_2$ [119]. Electrochemical studies show that both these 7 and 8-SEP Fe_3Rh species exhibit facile redox changes [119]. The position of the $2a_2$ MO at too low (near $3a_1$, see Fig. 5) or too high energy (near $2b_1$) renders difficult the possibility of having both 7 and 8-SEP counts for a given cluster. Field and coworkers have shown that

under CO pressure, the 7-SEP compounds $Ru_4(CO)_{10}L(\mu_4\text{-}PR)_2$ give products with more open geometry rather than the 8-SEP $closo$-octahedral cluster [141]. Electrochemical studies performed on 8-SEP $Co_4(CO)_{10-x}(PR_3)_x(\mu_4\text{-}PPh)_2$ by Richmond and Kochi reveal that the oxidation becomes more and more facile as the number of phosphine ligands increases [142]. It turns out that the replacement of CO groups by less π-acceptor phosphine ligands allows a noticeable destabilization of the weakly metal–metal antibonding $2a_2$ MO which houses the eighth SEP.

5.2. Two electrons more: nido-octahedral derivatives

A trigonal prismatic framework is expected for a count of 9 SEPs [1e]. $Ru_4(CO_{12}(\mu\text{-}H)_2(\mu_3\text{-}PPh)_2$ (44), which results from the conversion of a 7-SEP $closo$-octahedral $Ru_4(\mu_4\text{-}PPh)_2$ species by the addition of carbonyl and protons, provides us with a nice example of 9-SEP trigonal prismatic $M_4(\mu_3\text{-}E)_2$ cluster analogue to prismane C_6H_6 [143]. An alternative isomeric trigonal prismatic arrangement is that observed for the 9-SEP cluster $Ru_4(CO)_{11}(PPh)(\mu_4\text{-}\eta^2\text{-}N_2Ph_2)$ (45), in which the metallic square is capped on one side by the azobenzene group [144]. Note that (44) and (45) are electron-precise molecules. It appears that with more electronegative metal atoms, such an arrangement is in competition with the $nido$-pentagonal $M_4(\mu_4\text{-}E)_2$ bipyramid encountered in the 9-SEP compound $Co_4(CO)_3(F_2P)_2(NMe)_4(\mu_4\text{-}PPh)_2$ (46) for instance (see Table 4) [133]. The anticipated electron count for the latter geometry being only 8, cluster (46) does not conform to the Wade–Mingos rules.

44

45

46
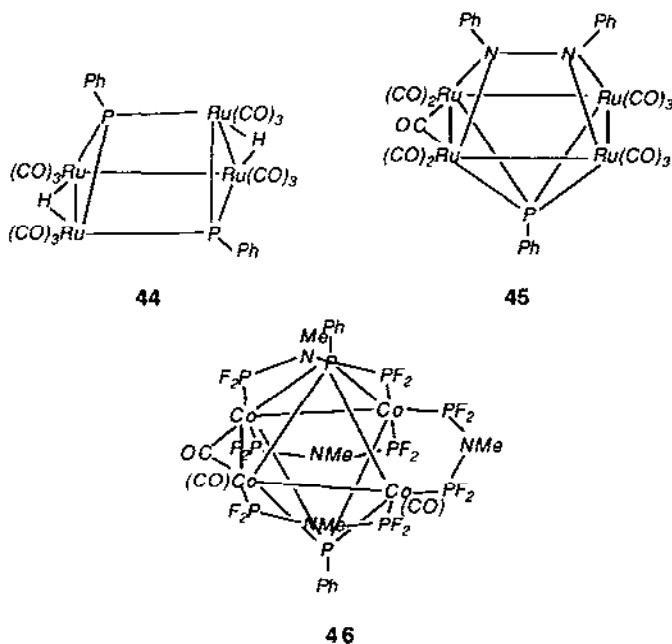
The opening of a metal–metal vector in the $M_4(\mu_4\text{-E})_2$ *closo*-octahedral species affords the *nido*-pentagonal-bipyramidal geometry. As illustrated on the right-hand side of Fig. 5, it brings about the stabilization of one metallic level ($2b_1$) which is now intercalated between the $3a_1$ and $2a_2$ MOs [145]. Only one important HOMO–LUMO gap subsists between the $2a_2$ and $4a_1$ MOs, favoring the unexpected count of 9 SEPs, in accord with the observed electron count of (46) and analogous species with Co_4Sb_2 and Co_4Bi_2 cores (see Table 4) [134,135].

This particular electron count, which differs from the predicted one by two electrons, is attributed, as in the case of the *closo* $M_4(\mu_4\text{-E})_2$ clusters, to electronic (the electronegativity nature) and geometric (the coplanarity) features of the four metal atoms brought into play. We have seen previously (Section 4.2) that the alternative isomeric $M_4(\mu_3\text{-E})_2$ geometry such as that of (40) [103] or that of analogues such as $Os_4(CO)_{12}(\mu_3\text{-S})_2$ (47) [146], in which the metal atoms form a butterfly array, leads to the expected electron count of 8 SEPs. This has been confirmed with EH calculations that we have carried out on $[Fe_4(CO)_{12}(\mu_3\text{-N})_2]^{2-}$ and $Os_4(CO)_{12}(\mu_3\text{-S})_2$ models [81,145].
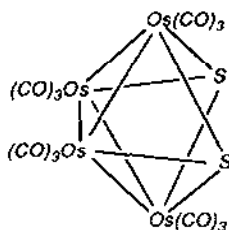
47

In the 7 and 8-SEP *closo*-octahedral $M_4(\mu_4\text{-E})_2$ compounds the difference in the covalent radii of M and E generally leads to a rather short contact between the two E atoms capping the metallic square (see Table 4 for the 8-SEP examples). The E···E separation, which is generally 12–20% longer than that expected for a single bond, is present not only because of steric demands, but also because the corresponding electronic interaction is significantly bonding. This recurring feature is observed, regardless of the count of 7 or 8 SEPs since the $2a_2$ MO does not possess any capping main group atom character [137]. The phosphorus–phosphorus separation measured in the 7-SEP $Fe_4(CO)_{10}(P(OMe)_3)(P\text{-}p\text{-Tol})_2$ and 8-SEP $Fe_4(CO)_{11}(P(OMe)_3)(P\text{-}p\text{-Tol})_2$ complexes, 2.646 Å and 2.598 Å, respectively, illustrates this particular feature [117].

For geometric reasons, the E···E contacts are even shorter in *nido*-pentagonal-bipyramidal $M_4(\mu_4\text{-E})_2$ complexes. A distance of 2.44 Å separates the two phosphorus atoms in the 9-SEP cobalt compound (46), only 10% longer than a P–P single bond. With heavier elements, distances comparable to a single bond are observed such as in $[Co_4(CO)_{11}(\mu_4\text{-Sb}_2)]^{2-}$ (48) and its bismuth analogue (see Table 4) [134]. EH calculations are in accord with this observation. The Sb–Sb overlap population computed in (48) is comparable to that computed in Sb_2H_4, a model used to mimic Sb_2Ph_4 in which the antimony atoms are singly bonded [147]. Another probe to

measure the E–E bonding is the occupation of the σ^* FMO of the E_2 moiety after interaction with the metallic fragment. The occupation will be close to zero if the E–E single bond exists, close to two if the E⋯E interaction does not exist. Hence the value of 0.27 which is computed in (**48**) reflects a strong Sb–Sb bonding interaction. The existence of an Sb–Sb bond in (**48**) led us to describe this 9-SEP *nido* structure in an alternative way [134]. Compound (**48**) can indeed be regarded as a Co_2Sb_2 tetrahedron with two $CoSb_2$ triangular faces capped by a $Co(CO)_3$ moiety. In accord with the PSEP rules, EH calculations have shown that a tetrahedral M_2E_2 cluster is consistent with a count of 6 SEPs [148]. The capping principle (see section 2) states that such a count of 6 SEPs should not change when one or two faces of the polyhedron are capped. This is the case of the 6-SEP bicapped-tetrahedral cluster $Os_6(CO)_{18}$ for instance, in which the FMOs of the $Os(CO)_3$ entities match in symmetry with low-lying FMOs of the $Os_4(CO)_{12}$ tetrahedron [149]. In (**48**) additional bonding interactions with high-lying "acceptor" FMOs of the Co_2Sb_2 tetrahedron prevent three FMOs of the capping $Co(CO)_3$ units being pushed sufficiently up in energy and being vacant [134]. Remaining at relatively low energy their occupation leads to the electron-rich count of 9 SEPs. Hence such a species does not conform to the capping principle.
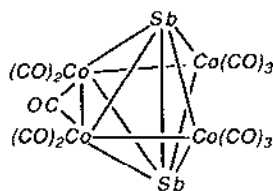
48

Both ways of looking (mentally) at 9-SEP electron-rich species (**48**) and its bismuth analogue, the *nido*-pentagonal bipyramid and the bicapped tetrahedron, are instructive. The former derivation, pointing out that relatively electronegative metal atoms should occupy the basal vertices of the *nido* bipyramid, shows immediately why only one skeletal isomer is encountered with such an electron count. The latter derivation, starting from a closed Co_2Sb_2 tetrahedral core, provides an explanation for the existence of a Sb–Sb bond.

5.3. Alternative geometries for M_4E_2 clusters

The different examples described above show that various M_4E_2 geometries can be adopted depending on their electron count and the nature of the metal atoms. In addition to the arrangements already mentioned, there is that reported for the 7-SEP cluster $Fe_3W(CO)_{11}(PMe_2Ph)(\mu_3-S)_2$ (**49**) in which two tetrahedra share a metal–metal edge [150]. Such a 7-SEP electron-precise structure consistent with the PSEP rules is an isomeric form of the *closo*-octahedral geometry. According to Fehlner and coworkers, this arrangement could depend on the ability of the "hinge" metal atoms to use more than three FMOs for cluster bonding [151].
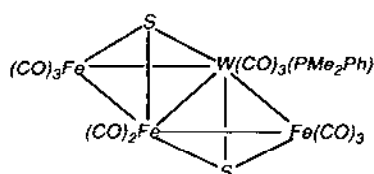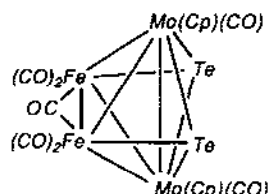
49   **50**

The 6-SEP bicapped-tetrahedral species $Fe_2Mo_2(Cp)_2(CO)_7(\mu_3\text{-}Te)_2$ **(50)** in which the Te atoms cap two $FeMo_2$ faces, provides a nice example of geometric isomer of compound **(48)** [152]. EH calculations carried out on such an alternative arrangement, where the main group atoms occupy the low connectivity sites rather than the high connectivity ones such as in **(48)**, give only one substantial HOMO–LUMO gap for the anticipated electron count of 6 SEPs [134,145]. This reflects the importantance of the preferred site occupation of the main group atoms in assigning the electron count in these types of structures. The same phenomenon, i.e. different electron counts with respect to the site occupations of the metal and main group atoms, has been noticed in dodecahedral metallaboranes [153].

5.4. Other examples of "rule-breakers"

Numerous examples of "rule-breaker" organometallic clusters adopting core geometries which belie the electron count are now found in the literature. In relation with those we have just discussed, let us mention the extensive class of the electron-rich tetrametallic molecules $Ru_4(CO)_{13}(\mu\text{-}PR_2)_2$ **(51)** having a rhomboidal Ru_4 core [154]. The actual electron count of these species, 8 SEPs or 64 CVEs, is two-electron richer than that anticipated with both the PSEP theory and the EAN formalism. The electrons in excess are then expected to populate an M–M antibonding MO leading to the cleavage of one metal–metal bond of one of the two triangles forming the rhombus. A global expansion of the metallic triangle spanned by the phosphido PR_2 groups is observed instead. EH calculations carried out by Carty, Mealli and colleagues on species **(51)**
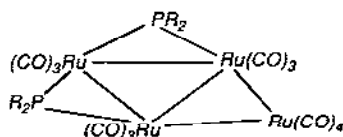
51

have indicated that the additional electrons are housed in an MO slightly antibonding with respect to the metallic triangle bridged by the PR_2 ligands [154,155]. This antibonding MO **(52a)** is, by symmetry, the full counterpart of an occupied bonding doubly degenerate e set **(52b)**. Consequently, its occupation completely removes the bonding effect of **(52b)**, and only two bonding electrons localized in a totally symmet-

ric MO (**52c**) remain to ensure the M–M bonding in this Ru_3 triangle. This leads to a formal M–M bond order of 1/3 (not 2/3 as one could erroneously deduce from the presence of only one extra electron pair in (**52a**)), in accord with the elongation of the M–M bonds. Such a two-electron three-center bonding scheme is reminiscent of that of $[H_3]^+$ [156].

52
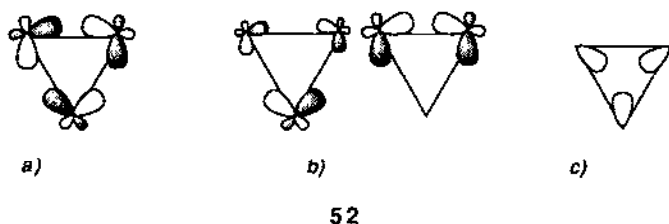
The same conclusions were reached in the case of 50-CVE trimetallic ruthenium compounds characterized by Lavigne's and Cabeza's groups [157,158]. Framework expansion rather than edge opening in these tetra- and trimetallic complexes seem to be borne out by the presence of two or more phosphido PR_2 bridges, since isoelectronic species with CO bridges adopt an open-triangle geometry consistent with the PSEP and the EAN rules [157]. According to Carty et al., the existence of these electron-rich complexes is due to the fact that bridging PR_2 groups are stronger donors than bridging CO ligands [154]. EH calculations that we performed on Lavigne's compounds agree with this statement [157]. This illustrates the fact that the ligands surrounding the core of the cluster are not simply electron-donor spectators.

The particular electronic effect of the ligands attached to the cluster core has also been noted in transition metal cyclopentadienyl clusters. Although the trigonal prismatic arrangement predicted by the Wade–Mingos rules would be sterically hindered, it is surprising somewhat that the 9-SEP (or 90-CVE) compound $Ni_6(Cp)_6$ (**53**) adopts a *closo*-octahedral geometry [159]. All the *closo*-octahedral M_6 compounds made of isolobal fragments have the anticipated count of 7 SEPs [137].

53
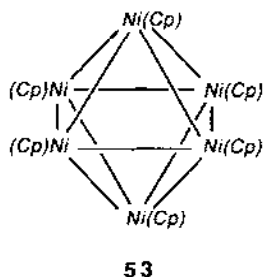
The origin of the failure of the PSEP rules to account for the geometry of (**53**) lies in the ligand versus metal composition of the FMOs of the conical Ni(Cp) fragment compared to that of $M(CO)_3$ [8]. We have seen previously that the comparison of the FMOs of the isolobal fragments $Fe(CO)_3$ and $[Fe(Cp)]^-$ shows a doubly degenerate π-type e FMO set more heavily distributed over the ligands in

the case of $[Fe(Cp)]^-$ (see Section 3.2). This is even more drastic with more electronegative metals such as Ni, since the e FMO set of $Ni(Cp)$ is less than 40% metallic in character (see Fig. 4) [160]. Consequently, when six $Ni(Cp)$ fragments are assembled together to form an octahedral geometry, some tangential out-of-phase combinations in which the ligand contribution prevails over that of nickel are not sufficiently meta–metal antibonding to be highly pushed up in energy. Therefore, they remain close enough to the M–M bonding and nonbonding MOs [160,161]. A partial occupation of a slightly M–M antibonding triply degenerate set of t_{2u} symmetry in the O_h symmetry group affords the count of 9 SEPs. The same situation is encountered in the 10-SEP *closo*-octahedral mixed cluster $Ni_4(Cp)_4(\mu_4\text{-Se})_2$ in which the "triply degenerate" MO set is fully occupied [136,160].

On the other hand, arene clusters generally obey the Wade–Mingos rules [162]. The fact that arene ligands are often associated with metal elements such as ruthenium or osmium, rather less electronegative than nickel, renders the FMOs of M(arene) fragments more heavily localized on the metal atom [8].

6. Concluding remarks

Despite its great success for understanding the structures of a large variety of organometallic clusters, the PSEP theory presents limitations which hamper its application to particular mixed main group–transition metal systems. In this review we have first outlined some of these failures to account for skeletal isomerism, isomer interconversion or unexpected geometries, which are in turn mainly due to the limitations of the isolobal analogy, and then have showed how molecular orbital calculations could help and sometimes circumvent these limitations.

Our study has been restricted to some tri- and tetrametallic clusters made of conical fragments. The scope could have been broader. We did not discuss, for instance, the isomerism present in square-pyramidal and octahedral arene clusters due to the different possible coordination modes of arene ligands [163]. We did not look at electron-deficient clusters violating the electron-counting rules such as the 7-SEP complex $[Ni_3Ru_3(CO)_{13}(\mu_6\text{-C})]^{2-}$ which adopts a *nido*-distorted octahedral geometry instead of the expected *closo*-octahedral structure [164]. We did not mention the clusters analogous to $Ni_8(CO)_8(\mu_4\text{-PPh})_6$ [165] which exhibit a large gamut of electron counts for the same cubic architecture [166]. Nevertheless, the diverse examples we have chosen to discuss here were able to illustrate that, to some extent, the PSEP rules embody relatively limited recognition of the large number of possible structures observed in cluster chemistry.

Questions remain. We started this review by mentioning osmium– and ruthenium–bismuth isomers (1) and (2) [2]. For instance, neither the PSEP rules nor the approximate EH calculations have explained so far the propensity of osmium and ruthenium to form butterfly and square frameworks, respectively [146,150,167]. Skeletal rearrangement mechanisms such as those discussed here are empirical and somewhat speculative, often being based on elusive experimental data and/or theoretical results obtained by a method notoriously unable to optimize the geometry of

the molecules. Clearly, a complete elucidation of fluxional processes in cluster chemistry requires more accurate experimental and theoretical investigations [168]. No doubt, in the near future, sophisticated quantum-mechanical calculations of ab initio or density functional type should be able to tackle these questions more quantitatively, thereby fostering a better understanding of the structural features of clusters and more rapid improvements of the PSEP theory [169,170].

Acknowledgment

Thanks are expressed to Professor J.-Y. Saillard for helpful comments.

References

[1] The term PSEP was first introduced by R. Mason, K.M. Thomas and D.M.P. Mingos, J. Am. Chem. Soc., 95 (1973) 3802. For a complete description of the PSEP theory see for instance: (a) K. Wade, Adv. Inorg. Chem. Radiochem., 18 (1976) 1. (b) K. Wade, in B.F.G. Johnson, (ed.), Transition Metal Clusters, Wiley, New York, 1981, p. 193. (c) D.M.P. Mingos, Acc. Chem. Res., 17 (1984) 311. (d) D.M.P. Mingos, R.L. Johnston, Struct. Bonding, 68 (1987) 29. (e) D.M.P. Mingos, D.J. Wales, Introduction to Cluster Chemistry, Prentice-Hall, Englewood Cliffs, NJ, 1990.
[2] (a) H.G. Ang, C.M. Hay, B.F. G. Johnson, J. Lewis, P.R. Raithby and A.J. Whitton, J. Organomet. Chem., 330 (1987) C5. (b) C.M. Hay, B.F.G. Johnson, J. Lewis, P.R. Raithby and A.J. Whitton, J. Chem. Soc. Dalton Trans., (1988) 2091.
[3] (a) R.C. Ryan and L.F. Dahl, J. Am. Chem. Soc., 97 (1975) 6904. (b) R.C. Ryan, C.U. Pittmann, J.P. O'Connor and L.F. Dahl, J. Organomet. Chem., 193 (1980) 247.
[4] See for example: (a) J.W. Lauher, J. Am. Chem. Soc., 100 (1978) 5305. (b) B. Teo, G. Longoni and F.R. Chung, Inorg. Chem., 24 (1984) 1257. (c) B. Teo, Inorg. Chem., 24 (1985) 1251. (d) R.B. King, New J. Chem., 12 (1988) 493 and references therein.
[5] K. Wade, J. Chem. Soc. Chem. Commun., (1971) 792.
[6] (a) R.E. Williams, Inorg. Chem., 10 (1971) 210. (b) R.E. Williams, Adv. Inorg. Chem. Radiochem., 18 (1976) 67. (c) R.W. Rudolph and W.R.Pretzer, Inorg. Chem., 11 (1972) 1974. (d) R.W. Rudolph, Acc. Chem. Res., 9 (1976) 446.
[7] (a) D.M.P. Mingos, Nature (Lond.) Phys. Sci., 236 (1972) 99. (b) K. Wade, Inorg. Nucl. Chem. Lett., 8 (1972) 559, 563, 823. (c) K. Wade, Nature (Lond.) Phys. Sci., 240 (1972 71.
[8] (a) M. Elian, M.L. Chen, D.M.P. Mingos and R. Hoffmann, R. Inorg. Chem., 15 (1976) 1148. (b) R. Hoffmann, Angew. Chem. Int. Edn. Engl., 21 (1982) 711.
[9] M. McPartlin, R.R. Eady, B.F. G. Johnson and J. Lewis, J. Chem. Soc. Chem. Commun., (1976) 883.
[10] R. Jackson, B.F.G. Johnson, J. Lewis, P.R. Raithby and S.W. Sankey, J. Organomet. Chem., 193 (1980) C1.
[11] (a) D.G. Evans and D.M.P. Mingos, J. Organomet. Chem., 240 (1982) 321. (b) D.G. Evans and D.M.P. Mingos, Organometallics, 2 (1983) 435.
[12] R.L. Johnston and D.M.P. Mingos, J. Organomet. Chem., 280 (1985) 407.
[13] D.M.P. Mingos and M.I. Forsyth, J. Chem. Soc. Dalton Trans., (1977) 610.
[14] D.M.P. Mingos, J. Chem. Soc. Chem. Commun., (1983) 706.
[15] (a) D.M.P. Mingos, J. Chem. Soc. Chem. Commun., (1985) 1352. (b) D.M.P. Mingos, Chem. Soc. Rev., 15 (1986) 31.
[16] (a) A.J. Stone, Mol. Phys., 41 (1980) 1339. (b) A.J. Stone, Inorg. Chem., 21 (1981) 563. (c) A.J. Stone and M.J. Alderton, Inorg. Chem., 21 (1982) 2297. (d) A.J. Stone, Polyhedron, 3 (1984) 2051. (e) D.J.Wales and A.J. Stone, Inorg. Chem., 28 (1989) 3120.

[17] (a) R. Hoffmann, J. Chem. Phys., 39 (1963) 1397. (b) R. Hoffmann and W.N. Lipscomb, J. Chem.
     Phys., 36 (1962) 2179, 3489; 37 (1962) 2872. (c) J.H. Ammeter, H.-B. Bürgi, J.C. Thibeault and R.
     Hoffmann, J. Am. Chem.Soc., 100 (1978) 3686.
[18] See for example: (a) E. Sappa, A. Tirripicchio and P. Braunstein, Chem.Rev., 83 (1983) 203. (b)
     M.I. Bruce, J. Organomet. Chem., 257 (1983)417. (c) E. Sappa, A. Tirripicchio and P. Braunstein,
     Coord. Chem. Rev., 65(1985) 219. (d) P.R. Raithby and M.J. Rosales, Adv. Inorg. Chem.
     Radiochem., 29 (1985) 169. (e) D. Osella and P.R. Raithby, in I. Bernal (ed.), Stereochemistry of
     Organometallic and Inorganic Compounds, Elsevier, Amsterdam, 1988, Vol. 3. (f) G. Lavigne in
     D.F. Shriver, H.D. Kaesz and R.D. Adams (eds.), The Chemistry of Metal Clusters, Verlag Chemie,
     Weinheim, 1990, p. 201.
[19] M.G. Thomas, E.L. Muetterties, R.O. Day and V.W. Day, J. Am. Chem.Soc., 98 (1976) 4645.
[20] J.F. Blount, L.F. Dahl, C. Hoogzand and W.J. Hübel, J. Am. Chem. Soc., 88 (1966) 292. See also:
     (a) A.J. Carty, N.J. Taylor and E. Sappa, Organometallics, 7 (1988) 405. (b) D. Osella, L. Pospisil
     and J. Fiedler, Organometallics, 12 (1993) 3140 and references therein.
[21] S. Aime, L. Milone, D. Osella, A. Tirripicchio and A.M.M. Lanfredi, Inorg. Chem., 21 (1982) 501.
[22] For exceptions see: R.S. Dickson and O.M. Paravagna, Organometallics, 10 (1991) 721.
[23] B.E. R. Schilling and R. Hoffmann, J. Am. Chem. Soc., 101 (1979) 3456.
[24] G. Granozzi, E. Tondello, M. Casarin, S. Aime and D. Osella, Organometallics, 2 (1983) 430.
[25] V. Busetti, G. Granozzi, S. Aime, R. Gobetto and D. Osella, Organometallics, 3(1984) 1510.
[26] J.-F. Halet, J.-Y. Saillard, R. Lissillour, M.J. McGlinchey and G. Jaouen, Inorg. Chem., 24(1985) 218.
[27] S. Aime, R. Bertoncello, V. Busetti, R. Gobetto, G. Granozzi and D. Osella, Inorg. Chem., 25
     (1986) 4004.
[28] Z. Nomikou, J.-F. Halet, R. Hoffmann, R.D. Adams and J.T. Tanner, Organometallics, 9 (1990) 588.
[29] L. Busetto, J.C. Jeffrey, R.M. Mills, F.G.A. Stone, M.J. Went and P. Woodward, J. Chem. Soc.
     Dalton Trans. (1983) 101.
[30] (a) L. Busetto, M. Green, J.A.K. Howard, B. Hessner, J.C. Jeffrey, R.M. Mills, F.G.A. Stone and P.
     Woodward, J. Chem. Soc. Chem. Commun. (1981) 1101. (b) L. Busetto, M. Green, B. Hessner,
     J.A.K. Howard, J.C. Jeffrey and F.G.A. Stone, J. Chem. Soc. Dalton Trans. (1983) 519.
[31] D. Boccardo, M. Botta, R. Gobetto and D. Osella, J. Chem. Soc. Dalton Trans. (1988) 1249.
[32] (a) M.I. Bruce, J.R. Rodgers, M.R. Snow and F.S. Wong, J. Chem. Soc. Chem. Commun. (1980)
     1285. (b) M.I. Bruce, J.R. Rodgers, M.R. Snow and F.S. Wong, J. Organomet. Chem., 240 (1982) 299.
[33] (a) G. Jaouen, A. Marinetti, B. Mentzen, R. Mutin, J.-Y. Saillard, B.G. Sayer and M.J. McGlinchey,
     Organometallics, 1 (1982) 753. (b) M. Mlekuz, P. Bougeard, B.G. Sayer, S. Peng, M.J. McGlinchey,
     A. Marinetti, J.-Y.Saillard, J. Ben Naceur, B. Mentzen and G. Jaouen, Organometallics, 4
     (1985)1123.
[34] (a) F.W. Einstein, K.G. Tyers, D. Sutton and J.M. Waterous, J. Chem. Soc. Chem. Commun. (1982)
     371. (b) F.W. Einstein, B.H. Freeland, K.G. Tyers, A.S. Tracey and D. Sutton, Inorg. Chem., 25
     (1986) 1631.
[35] E. Sappa, A.M. M. Lanfredi and A. Tirripicchio, J. Organomet. Chem., 221(1981) 93.
[36] H. Bantel, A.K. Powell, and H. Vahrenkamp, Chem. Ber., 123 (1990) 1607.
[37] P. Braunstein, J. Rosé and O. Bars, J. Organomet. Chem., 252 (1983) C101.
[38] H. Bantel, W. Bernhardt, A.K. Powell and H. Vahrenkamp, Chem. Ber., 121 (1988) 1247.
[39] E. Sappa, A. Tirripicchio and M. Tirripicchio-Camellini, J. Organomet. Chem., 213 (1981) 175.
[40] M.I. Bruce, G.A. Koutsantonis and E.R.T. Tiekink, J. Organomet. Chem., 407 (1991) 391.
[41] M.R. Churchill, C. Bueno and J.J. Wasserman, Inorg. Chem., 21 (1982) 640.
[42] M.J. McGlinchey, in Topics in Physical Organometallic Chemistry, M. Gielen (ed.), Vol. 4, 1992,
     p. 41.
[43] A.L. Allred and E.G. Rochow, J. Inorg. Nucl. Chem., 5 (1958) 264, 269.
[44] A.J. Deeming, J. Organomet. Chem., 150 (1978) 123.
[45] M.J. McGlinchey, M. Mlekuz, P. Bougeard, B.G. Sayer, A. Marinetti, J.-Y. Saillard and G. Jaouen,
     Can. J. Chem., 61 (1983) 1319.
[46] B.E.R. Schilling and R. Hoffmann, Acta Chem. Scand., B33 (1979) 231.
[47] W.-D. Stohrer and R. Hoffmann, J. Am. Chem. Soc., 94 (1972) 779.
[48] (a) R. Rumin, F.Y. Pétillon, A.H. Anderson, Lj. Manojlovic-Muir and K.W. Muir, J. Organomet.

Chem., 336 (1987) C50. (b) R. Rumin, F.Y. Pétillon, Lj. Manojlovic-Muir and K.W. Muir, Organometallics, 9 (1990) 944.

[49] R. Rumin, F. Robin-Le Guen, J. Talarmin and F.Y. Pétillon, Organometallics, 13 (1994) 1155.

[50] R.D. Adams and J.T. Tanner, Organometallics, 7 (1988) 2241.

[51] A.J. Deeming, A.S.E. Kabir, D. Nuel and N.I. Powell, Organometallics, 8 (1989)717.

[52] (a) R.S. Dickson, O.M. Paravagna and H. Pateras, Organometallics, 9(1990) 2780. (b) R.S. Dickson, Polyhedron, 10 (1991) 1995.

[53] For a review on aminoacetylenes (also known as ynamines) contained in organometallic clusters see: R.D. Adams, J.-C. Daran and Y. Jeannin, J. Cluster Sci., 3 (1992) 1 and references therein.

[54] R.J. Goudsmit, B.F. G. Johnson, J. Lewis, P.R. Raithby and M.J. Rosales, J. Chem. Soc. Dalton Trans. (1983) 2257.

[55] E. Boyar, A.J. Deeming, M.S.B. Felix, S.E. Kabir, T. Adatia, R. Bhusate, M. McPartlin and H.R. Powell, J. Chem. Soc. Dalton Trans. (1989)5.

[56] M.R. Churchill, J.C. Fettinger, J.B. Keister, R.F. See and J.W. Ziller, Organometallics, 4 (1985) 2112.

[57] A.J. Deeming, A.J. Arce, Y. De Sanctis, M.W. Day and K.I. Hardcastle, Organometallics, 8 (1989) 1408.

[58] R.D. Adams, G. Chen and J. Tanner, Organometallics, 9 (1990) 1530.

[59] M. Day, S. Hajela, K.I. Hardcastle, T. McPhillips, E. Rosenberg, M. Botta, R.Gobetto, L. Milone, D. Osella and R.W. Gellert, Organometallics, 9 (1990) 913.

[60] R.D. Adams, G. Chen, J. Tanner and J. Yin, Organometallics, 9 (1990) 1240.

[61] R.D. Adams, G. Chen, T.J. Tanner and J. Yin, Organometallics, 8 (1989) 2493. See also: R.D. Adams, G. Chen, S. Sun, T.J. Tanner and T.A. Wolfe, Organometallics, 9 (1990) 251.

[62] R.D. Adams, J.E. Babin, M. Tasi and T.A. Wolfe, Organometallics. 6 (1987) 2228. See also: (a) A.J. Deeming, N.I. Powell, A.J. Arce, Y. De Sanctis and J. Manzur, J. Chem. Soc. Dalton Trans. (1991) 3381. (b) R.D. Adams, G. Chen, X. Qu, W. Wu and J.H. Yamamoto, Organometallics, 12 (1993) 3029. (c) R.D. Adams, X. Qu and W. Wu, Organometallics, 12 (1993) 4117. (d) R.D. Adams, T.S. Barnard, Z. Li, W. Wu and J. Yamamoto, Organometallics, 13 (1994) 2357.

[63] R.B. King and C. Darmon, Inorg. Chem., 15 (1976) 879.

[64] J.R. Fritch, K.P.C. Vollhardt, M.R. Thompson and V.W. Day, J. Am. Chem.Soc., 101 (1979) 2768.

[65] J.R. Fritch and K.P.C. Vollhardt. Angew. Chem. Int. Ed. Engl., 19 (1980) 559.

[66] N.T. Allison, J.R. Fritch, K.P.C. Vollhardt and E.C. Walborsky, J. Am. Chem.Soc., 105 (1983) 1384.

[67] A.D. Clauss, J.R. Shapley, C.N. Wilker and R. Hoffmann, Organometallics, 3(1984) 619.

[68] (a) D. Lentz, I. Brüdgam and H. Hartl, Angew. Chem. Int. Ed. Engl., 24 (1985)119. (b) D. Lentz and H. Michael, Inorg. Chem., 28 (1989) 3396.

[69] Y. Chi and J.R. Shapley, Organometallics, 4 (1985) 1900.

[70] D. Nuel, F. Dahan and R. Mathieu, Organometallics, 4 (1985) 1436.

[71] B. Eaton, J.M. O'Connor and K.P. C. Vollhardt, Organometallics, 5 (1986) 394.

[72] J. Hriljac and D.F. Shriver, J. Am. Chem. Soc., 109 (1987) 6010.

[73] E. Cabrera, J.-C. Daran and Y. Jeannin, J. Chem. Soc. Chem. Commun. (1988)607.

[74] P. Quénec'h, R. Rumin and F.Y. Pétillon, J. Organomet. Chem., 479 (1994) 93.

[75] (a) E. Wucherer and H. Vahrenkamp, Angew. Chem. Int. Ed. Engl., 26 (1987)355. (b) M. Tasi, A.K. Powell and H. Vahrenkamp, Angew. Chem. Int. Ed. Engl., 28 (1989) 318.

[76] E. Wucherer, M. Tasi, B. Hansert, A.K. Powell, M.T. Garland, J.-F. Halet, J.-Y. Saillard and H. Vahrenkamp, Inorg. Chem., 28 (1989) 3564.

[77] M.P. Jensen and D.F. Shriver, Organometallics, 11 (1992) 3385.

[78] H. Bantel, B. Hansert, A.K. Powell, M. Tasi and H. Vahrenkamp, Angew. Chem. Int. Ed. Engl., 28 (1989) 8.

[79] R.L. DeKock, P. Deshmukh, T.K. Dutta, T.P. Fehlner, C.E. Housecroft and J.L.-S. Hwang, Organometallics, 2 (1983) 1108.

[80] (a) G. Granozzi, R. Bertoncello, M. Acampora, D. Ajò, D. Osella and S. Aime, J. Organomet. Chem., 244 (1983) 383. (b) D. Osella, M. Ravera, C. Nervi, C.E. Housecroft, P.R. Raithby, P. Zanello and F. Laschi, Organometallics, 10 (1991) 3253.

[81] S. Kahlal, J.-F. Halet and J.-Y. Saillard, New J. Chem., 15 (1991) 843.

[82] L. Dieter and M. Heike, Angew. Chem. Int. Ed. Engl., 27 (1988) 27.

[83] T. Albriez, A.K. Powell and H. Vahrenkamp, Chem. Ber., 123 (1990) 667.

[84] S. Aime, L. Milone, D. Osella, A.M. Manotti Lanfredi and A. Tiripicchio, Inorg. Chim. Acta, 71 (1983) 141.

[85] E. Sappa, D. Belletti, A. Tiripicchio and M. Tiripicchio Camellini, J. Organomet. Chem., 359 (1989) 419.

[86] J.F. Fox, W.L. Gladfelter, G.L. Geoffroy, I. Tavanaiepour, S. Abdel-Mequid and V.W. Day, Inorg. Chem., 20 (1981) 3230.

[87] H. Bantel, A.K. Powell and H. Vahrenkamp, Chem. Ber., 123 (1990) 677.

[88] H.T. Schacht and H. Vahrenkamp, Chem. Ber., 122 (1989) 2239.

[89] F. Robin, R. Rumin, F.Y. Pétillon, K. Foley and K.W. Muir, J. Organomet. Chem., 418 (1991) C33.

[90] D.F. Jones, P.H. Dixneuf, A. Benoit and J.-Y. Le Marouille, J. Chem. Soc. Chem. Commun. (1982) 1217.

[91] G.F. Stuntz, J.R. Shapley and C.G. Pierpont, Inorg. Chem., 17 (1978) 9.

[92] I.T. Horvath, L. Zsolnai and G. Huttner, Organometallics, 5 (1986) 180.

[93] I. Ojima, N. Clos, R.J. Donavan and P. Ingallina, Organometallics, 10 (1991) 3211.

[94] S.P. Tunik, V.R. Krym, G.L. Starova, A.B. Nikol'skii, I.S. Podkorytov, S. Ooi, M. Yamasaki and M. Shiro, J. Organomet. Chem., 481 (1994) 83.

[95] A.D. Shaposhnikova, G.L. Kamalov, R.A. Stadnichenko, A.A. Pasynskii, I.L. Eremenko, S.E. Nefedov, Yu.T. Struchkov and A.I. Yanovsky, J. Organomet. Chem., 405 (1991) 111.

[96] A.D. Shaposhnikova, R.A. Stadnichenko, V.K. Belsky and A.A. Pasynskii, Izv. Akad. Nauk SSSR, Ser. Khim., 8 (1987) 1913 (Bull. Acad. Sci. USSR Div. Chem. Sci, 36 (1988) 1776).

[97] A.T. Brooker, P.A. Jackson, B.F. G. Jonhson, J. Lewis and P.R. Raithby, J. Chem. Soc. Dalton Trans. (1991) 707.

[98] J.-F. Halet, in Topics in Physical Organometallic Chemistry, M. Gielen (ed.), Vol. 4, 1992, p. 221 and references therein.

[99] J.A. Hriljac, S. Harris and D.F. Shriver, Inorg. Chem., 27 (1988) 816.

[100] (a) J.T. Park, J.R. Shapley, C. Bueno, J.W. Zeller and M.R. Churchill, J. Am. Chem. Soc., 105 (1983) 6182. (b) J.T. Park, J.R. Shapley, C. Bueno, J.W. Zeller and M.R. Churchill, Organometallics, 7 (1988) 2307. See also U. Riaz, M.D. Curtis, A. Rheingold and B.S. Haggerty, Organometallics, 9 (1991) 2647.

[101] E. Keller and D. Wolters, Chem. Ber., 117 (1984) 1572.

[102] E. Sappa, A.M. Manotti Lanfredi, G. Predieri, A. Tiripicchio and A.J. Carty, J. Organomet. Chem., 288 (1985) 365. See also: (a) J.-C. Daran, Y. Jeannin and O. Kristiansson, Organometallics, 4 (1984) 1882. (b) J. Luniss, S.A. MacLaughlin, N.J. Taylor and A.J. Carty, Organometallics, 4 (1984) 2066. (c) M.L. Blohm, W.L. Gladfelter, J.-C. Daran, Y. Jeannin and O.Kristiansson, Organometallics, 5 (1985) 1049. (d) J.F. Corrigan, S.Doherty, N.J. Taylor and A.J. Carty, Organometallics, 12 (1993) 1365.

[103] J.-S. Song, S.-H. Han, S.T. Nguyen, G.L. Geoffroy and A.L. Rheingold, Organometallics, 9 (1990) 2386.

[104] B. Hansert, A.K. Powell and H. Vahrenkamp, Chem. Ber., 124 (1991) 2697. See also B. Hansert and H. Vahrenkamp, Chem. Ber., 126 (1993) 2023.

[105] P. Jutzi, R. Kroos, A. Müller and M. Penk, Angew. Chem. Int. Ed. Engl., 28 (1989) 600.

[106] (a) B.F.G. Johnson, J. Chem. Soc. Chem. Commun. (1986) 27. (b) A. Rodger and B.F.G. Johnson, Polyhedron, 7 (1988) 1107.

[107] See for example: (a) J.R. Shapley, C.H. McAteer, M.R. Churchill and L.V. Biondi, Organometallics, 3 (1984) 1595. (b) R. Rumin, F. Robin, F.Y.Pétillon, K.W. Muir and I. Stevenson, Organometallics, 10 (1991) 2274. (c) A.D. Shaposhnikova, M.V. Drab, G.L. Kamalov, A.A. Pasynskii, I.L. Eremenko, S.E. Nefedov, Yu.T. Struchkov and A.I. Yanovsky, J. Organomet. Chem., 429 (1992) 109. (d) J.T. Park, B. Won Woo, J.-H. Chung, S. Chul Shim, J.-H. Lee, S.-S. Lim and I.-H. Suh, Organometallics, 13 (1994) 3384.

[108] S. Kahlal, J.-F. Halet and J.-Y. Saillard, Inorg. Chem., 30 (1991) 2567.

[109] (a) C.S. Jun, T.P. Fehlner and A.L. Rheingold, J. Am. Chem. Soc., 115 (1993) 4393. (b) C.S. Jun, J.-F. Halet, A.L. Rheingold and T.P. Fehlner, Inorg. Chem., 34 (1995) 2101.

[110] For 7-SEP octahedral $M_4(\mu_4\text{-E})_2$ examples, see for instance: (a) R.D. Adams and M. Tasi, J. Cluster

Sci., 1 (1990) 49. (b) P. Mathur, M.M. Hossain and R.S. Rashid, J. Organomet. Chem., 467 (1994) 245 and references therein.

[111] S.G. Anema, S.K. Lee, K.M. Mackay and B.K. Nicholson, J. Organomet. Chem., 444 (1993) 211.

[112] M. Van Tiel, K.M. Mackay and B.K. Nicholson, J. Organomet. Chem., 326 (1987) C101.

[113] S.P. Foster, K.M. Mackay and B.K. Nicholson, J. Chem. Soc. Chem. Commun. (1982) 1156.

[114] S.G. Anema, S.K. Lee, K.M. Mackay, L.C. McLeod, B.K. Nicholson and M. Service, J. Chem. Soc. Dalton Trans. (1991) 1209.

[115] S.P. Foster, K.M. Mackay and B.K. Nicholson, Inorg. Chem., 24 (1985) 909.

[116] P. Gusbeth and H. Vahrenkamp, Chem. Ber., 118 (1985) 909.

[117] (a) H. Vahrenkamp and D. Wolters, Organometallics, 1 (1982) 874. (b) T. Jaeger, S. Aime and H. Vahrenkamp, Organometallics, 5 (1986) 245.

[118] H. Vahrenkamp, E.J. Wucherer and D. Wolters, Chem. Ber., 116 (1983) 1219.

[119] H.H. Ohst and J.K. Kochi, Organometallics, 5 (1986) 1359.

[120] H. Vahrenkamp and M. Müller, Chem. Ber., 116 (1983) 2765.

[121] M.-J. Don, M.G. Richmond, W.H. Watson and A. Nagl, Acta Crystallogr., C47 (1991) 93.

[122] M.G. Richmond and J.K. Kochi, Organometallics, 6 (1987) 777.

[123] M.G. Richmond and J.K. Kochi, Inorg. Chem., 25 (1986) 1334.

[124] M.-J. Don, M.G. Richmond, W.H. Watson and A. Nagl, Acta Crystallogr., C45 (1989) 736.

[125] M.G. Richmond and J.K. Kochi, Organometallics, 6 (1987) 254.

[126] C.L. Schulman, M.G. Richmond, W.H. Watson and A. Nagl, J. Organomet. Chem., 368 (1989) 367.

[127] M.-J. Don, M.G. Richmond, W.H. Watson and A. Nagl, J. Organomet. Chem., 372 (1989) 417.

[128] J. Queisser and D. Fenske, Z. Anorg. Allg. Chem., 620 (1994) 58.

[129] A.M. Arif, A.H. Cowley, M. Pakulski, M.B. Hursthouse and A. Karauloz, Organometallics, 5, (1985) 2227.

[130] H. Vahrenkamp and E.J. Wucherer, Angew. Chem. Int. Ed. Engl., 20 (1981) 680.

[131] C.H. Wei and L.F. Dahl, Cryst. Struct. Commun., 4 (1975) 583.

[132] F. Jiang, X. Lei, Z. Huang, M. Hong, B. Kang, D. Wu and H. Liu, J. Chem. Soc. Chem. Commun. (1990) 1655.

[133] (a) M.G. Richmond, J.D. Korp and J.K. Kochi, J. Chem. Soc. Chem. Commun. (1985) 1102. (b) M.G. Richmond and J.K. Kochi, Inorg. Chem., 26 (1987) 541.

[134] (a) J.S. Leigh, K.H. Whitmire, K.A. Yee and T.A. Albright, J. Am. Chem.Soc., 111 (1989) 2726. (b) T.A. Albright, K.A. Yee, J.-Y. Saillard, S. Kahlal, J.-F. Halet, J.S. Leigh and K.H. Whitmire, Inorg. Chem., 30 (1991) 1179.

[135] S. Martinengo and G. Ciani, J. Chem. Soc. Chem. Commun. (1987) 1589.

[136] D. Fenske, A. Hollnagel and K. Merzweiler, Angew. Chem. Int. Ed. Engl., 27 (1988) 965.

[137] J.-F. Halet, R. Hoffmann and J.-Y. Saillard, Inorg. Chem., 25 (1985) 1695.

[138] R.D. Adams, J.E. Babin, J. Estradia, J.-G. Wang, M.B. Hall and A.A. Low, Polyhedron, 8 (1989) 1885.

[139] S.N. Datta, R.-K. Kondru and P. Mathur, J. Organomet. Chem., 470 (1994) 169.

[140] T. Feng, P. Lau, W. Imhof and G. Huttner, J. Organomet. Chem., 414 (1991) 89. See also: D. Eber, G. Huttner, D. Günauer, W. Imhof and L. Zsolnai, J. Organomet. Chem., 414 (1991) 361.

[141] J.S. Field, R.J. Haines, D.N. Smit, K. Natarajan, O. Scheidsteger and G. Huttner, J. Organomet. Chem., 240 (1982) C23.

[142] M.G. Richmond and J.K. Kochi, Inorg. Chem., 25 (1986) 656.

[143] J.S. Field, R.J. Haines, U. Honrath and D.N. Smit, J. Organomet. Chem., 329 (1987) C25.

[144] J.F. Corrigan, S. Doherty, N.J. Taylor and A.J. Carty, J. Chem. Soc. Chem. Commun. (1991) 1640. See also for alkyne analogue: J.F. Corrigan, N.J. Taylor and A.J. Carty, Organometallics, 13 (1994) 3778.

[145] J.-F. Halet and J.-Y. Saillard, New J. Chem., 11 (1987) 315.

[146] R.D. Adams, Polyhedron, 4 (1985) 2003.

[147] K. Van Deuter and D. Rehder, Cryst. Struct. Commun., 9 (1980) 167.

[148] J.-F. Halet and J.-Y. Saillard, J. Organomet. Chem., 327 (1987) 365 and references therein.

[149] R. Mason, K.M. Thomas and D.M.P. Mingos, J. Am. Chem. Soc., 95 (1973) 3802.

[150] R.D. Adams, J.E. Babin, J.-G. Wang and W. Wu, Inorg. Chem., 28 (1989) 703.

[151] T.P. Fehlner, C.E. Housecroft and K. Wade, Organometallics, 2 (1983) 1426.
[152] L.E. Bogan Jr., T.B. Rauchfuss and A.L. Rheingold, J. Am. Chem. Soc., 107 (1985) 3843. See also:
      P. Mathur, M.M. Hossain and A.L. Rheingold, Organometallics, 13 (1994) 3909.
[153] R.N. Grimes, Pure Appl. Chem., 54 (1982) 43 and references therein. For a theoretical study see:
      (a) D.N. Cox, D.M. P. Mingos and R. Hoffmann, J. Chem. Soc. Dalton Trans. (1981) 1788. (b)
      T.P. Fehlner, J.Organomet. Chem., 478 (1994) 49.
[154] (a) G. Hogarth, J.A. Phillips, F. Van Castel, N.J. Taylor, T.B. Marder and A.J. Carty, J. Chem.
      Soc. Chem. Commun. (1988) 1570. (b) J.F. Corrigan, Y. Sun, A.J. Carty, New J. Chem., 18 (1994)
      77. (c) J.F. Corrigan, M. Dinardo, S. Doherty, G. Hogarth, Y. Sun, N.J. Taylor and A.J.Carty,
      Organometallics, 13 (1994) 3572.
[155] C. Mealli and D. Proserpio, J. Am. Chem. Soc., 112 (1990) 5484.
[156] T.A. Albright, J.K. Burdett and M.-H. Whangbo, Orbital Interactions in Chemistry, Wiley, New
      York, 1985.
[157] N. Lugan, P.-L. Fabre, D. de Montauzon, G. Lavigne, J.-J. Bonnet, J.-Y. Saillard and J.-F. Halet,
      Inorg. Chem., 32 (1992) 1363.
[158] J.A. Cabeza, R.J. Franco, A. Llamazares, V. Riera, E. Pérez-Carreño and J.F. Van der Maelen,
      Organometallics, 13 (1994) 55.
[159] M.S. Paquette and L.F. Dahl, J. Am. Chem. Soc., 102 (1980) 6623.
[160] S. Kahlal, J.-F. Halet and J.-Y. Saillard, unpublished results.
[161] C. Mealli, J.A. Lopez, Y. Sun and M.J. Calhorda, Inorg. Chim. Acta, 213, (1993) 199.
[162] D. Braga, P.J. Dyson, F. Grepioni and B.F.G. Johnson, Chem. Rev., 94 (1994) 1585 and
      references therein.
[163] D. Braga, P.J. Dyson, F. Grepioni, B.F.G. Johnson and M.J. Calhorda, Inorg. Chem., 33
      (1994) 3218.
[164] M.P. Jensen, W. Henderson, D.H. Johnston, M. Sabat and D.F. Shriver, J. Organomet. Chem.,
      394 (1990) 121.
[165] L.D. Lower and L.F. Dahl, J. Am. Chem. Soc., 98 (1976) 5046.
[166] E. Furet, A. Le Beuze, J.-F. Halet and J.-Y. Saillard, J. Am. Chem. Soc., 116 (1994) 274.
[167] See for example: (a) R.D. Adams and M. Tasi, J. Cluster Sci., 1 (1990) 249.(b) R.D. Adams, T.A.
      Wolfe and W. Wu, Polyhedron, 10 (1991) 447.
[168] L. Girard, P.E. Lock, H. El Hamouri and M.J. McGlinchey, J. Organomet. Chem., 478 (1994) 189.
[169] J.-F. Riehl, N. Koga and K. Morokuma, Organometallics, 12 (1993) 4788 and references therein.
[170] T. Ziegler, Chem. Rev., 91 (1991) 651 and references therein.